Electronically competing phases and their magnetic field dependence in electron-doped nonsuperconducting and superconducting $Pr_{0.88}LaCe_{0.12}CuO_{4\pm\delta}$

H. J. Kang

Department of Physics and Astronomy, The University of Tennessee, Knoxville, Tennessee 37996-1200, USA

Pengcheng Dai*

Department of Physics and Astronomy, The University of Tennessee, Knoxville, Tennessee 37996-1200, USA
and Condensed Matter Sciences Division, Oak Ridge National Laboratory, Oak Ridge, Tennessee 37831-6393, USA

H. A. Mook

Condensed Matter Sciences Division, Oak Ridge National Laboratory, Oak Ridge, Tennessee 37831-6393, USA

D. N. Argyriou and V. Sikolenko

Hahn-Meitner-Institut, Glienicker Str 100, Berlin D-14109, Germany

J. W. Lynn

NIST Center for Neutron Research, National Institute of Standards and Technology, Gaithersburg, Maryland 20899, USA

Y. Kurita, Seiki Komiya, and Yoichi Ando

Central Research Institute of Electric Power Industry, Komae, Tokyo 201-8511, Japan

We present comprehensive neutron scattering studies of nonsuperconducting and superconducting electron-doped $Pr_{0.88}LaCe_{0.12}CuO_{4\pm\delta}$ (PLCCO). At zero field, the transition from antiferromagnetic (AF) as-grown PLCCO to superconductivity without static antiferromagnetism can be achieved by annealing the sample in pure Ar at different temperatures, which also induces an epitaxial $(Pr,La,Ce)_2O_3$ phase as an impurity. When the superconductivity first appears in PLCCO, a quasi-two-dimensional (2D) spin-density-wave (SDW) order is also induced, and both coexist with the residual three-dimensional (3D) AF state. A magnetic field applied along the $[\bar{1},1,0]$ direction parallel to the CuO_2 plane induces a "spin-flop" transition, where the noncollinear AF spin structure of PLCCO is transformed into a collinear one. The spin-flop transition is continuous in semiconducting PLCCO, but gradually becomes sharp with increasing doping and the appearance of superconductivity. A c-axis aligned magnetic field that suppresses the superconductivity also enhances the quasi-2D SDW order at (0.5,0.5,0) for underdoped PLCCO. However, there is no effect on the 3D AF order in either superconducting or nonsuperconducting samples. Since the same field along the $[\bar{1},1,0]$ direction in the CuO_2 plane has no (or little) effect on the superconductivity, (0.5,0.5,0) and $(Pr,La,Ce)_2O_3$ impurity positions, we conclude that the c-axis field-induced effect is intrinsic to PLCCO and arises from the suppression of superconductivity.

I. INTRODUCTION

All high-transition-temperature (high-T_c) copper oxides (cuprates) have insulating antiferromagnetic (AF), superconducting (SC), and metallic phases.[1] Understanding the nature of these coexisting and competing phases is a key challenge of current research in high-T_c superconductivity.[2,3] While the SC phase in cuprates arises from hole (p-type) or electron (n-type) doping of the insulating AF phase, it is still unclear how the superconductivity is related to the AF phase.[2]

In the hole-doped $La_{2-x}Sr_xCuO_4$ (LSCO) near $x \sim 1/8$ (Ref. 4) and La_2CuO_{4+y},[5] neutron scattering experiments have revealed the presence of a static incommensurate spin-density-wave (SDW) order in coexistence with the superconductivity. The SDW is quasi-two-dimensional (2D) with long-range order in the CuO_2 plane and short-range correlations along the c axis.[4,5] Indexed on a tetragonal unit cell of

LSCO, where the AF order occurs at the reciprocal lattice position (0.5,0.5) in the CuO_2 plane, the positions of the four incommensurate SDW peaks are $(0.5 \pm \Delta H, 0.5)$ and $(0.5, 0.5 \pm \Delta K)$ as shown in Fig. 1(b).[1] At optimal doping (highest T_c), the static SDW order in LSCO vanishes and is replaced by the appearance of a spin gap and incommensurate spin fluctuations at energies above the gap.[6] On the other hand, experiments on lightly doped insulating ($x=0.03, 0.04, 0.05$) and underdoped SC ($x=0.06$) LSCO have shown that the static SDW order appears in these samples, but intriguingly the four incommensurate peaks in Fig. 1(b) are only observed with the establishment of the bulk superconductivity for the underdoped SC samples ($0.06 \le x \le 0.12$).[7–9] Therefore, the insulating-to-superconducting phase transition induced by increasing hole(Sr)-doping is associated with the appearance of a static quasi-2D SDW modulation.
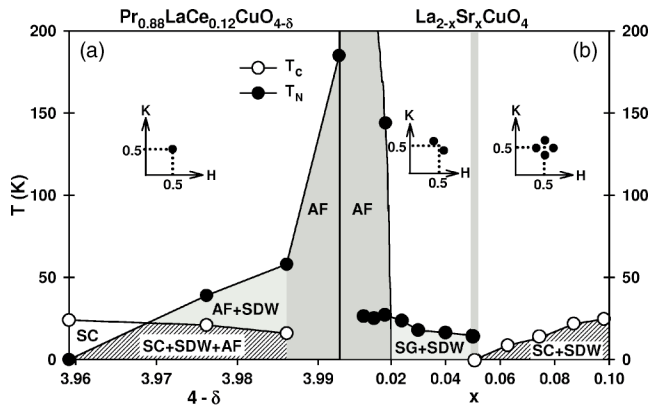
FIG. 1. Comparison of the phase diagrams between hole-doped $La_{2-x}Sr_xCuO_4$ (LSCO) and electron-doped $Pr_{0.88}LaCe_{0.12}CuO_{4\pm\delta}$ (PLCCO). (a) Properties of the PLCCO samples investigated in this work. Since the exact oxygen concentrations in our samples are unknown, the values of $4-\delta$ in the horizontal axis are obtained using Fig. 8 of Ref. 32 by assuming that PLCCO samples with the same T_c's as those of $Nd_{1.85}Ce_{0.15}CuO_{4-\delta}$ have the same oxygen content. When superconductivity is first established in PLCCO, a commensurate static SDW order also appears. The open and filled circles are data from Ref. 36. (b) Phase diagram of LSCO as a function of Sr doping from neutron scattering results of Refs. 7–9. In the spin-glass (SG) phase of LSCO, two static incommensurate SDW peaks at $(0.5+\Delta H, 0.5-\Delta K)$ and $(0.5-\Delta H, 0.5+\Delta K)$ (see inset) are observed for $0.02 \leqslant x \leqslant 0.05$. When superconductivity sets in at $x \geqslant 0.05$, two pairs of incommensurate SDW peaks appear simultaneously at $(0.5\pm\Delta H, 0.5)$ and $(0.5, 0.5\pm\Delta K)$. The data in (b) are from Refs. 7–9.

When a magnetic field is applied along the c-axis of the underdoped SC LSCO, it not only suppresses the superconductivity but also enhances the zero-field SDW order.[10–13] For optimally doped LSCO without static SDW order, a c-axis magnetic field induces spin fluctuations below the spin-gap energy and drives the system toward static AF order.[14,15] Since the same field applied in the CuO_2 plane has little effect on superconductivity or the SDW order,[16] these results suggest that antiferromagnetism is a competing ground state revealed by the suppression of superconductivity.[17–23]

If suppression of superconductivity in hole-doped LSCO indeed drives the system toward an AF ordered state, it is important to determine the universality of such a feature in other SC copper oxides.[24] Although neutron scattering experiments failed to confirm any enhancement of the static long-range AF order in hole-doped $YBa_2Cu_3O_{6.6}$ for a c-axis-aligned field up to 7 T,[25,26] these measurements may not be conclusive because of the enormous upper critical fields B_{c2} (>45 T for c-axis aligned fields) required to completely suppress superconductivity. Compared to hole-doped cuprates, electron-doped materials offer a unique opportunity for studying the magnetic field-induced effect for two reasons. First, electron-doped materials generally have upper critical fields less than 15 T,[27–29] a value reachable in neutron scattering experiments. Second, electron-doped materials can be transformed from as-grown nonsuperconducting (NSC) AF insulators to full superconductivity by simply annealing

the samples at different temperatures to modify the charge carrier density.[30–34] This unique property allows the possibility of studying the NSC to SC transition in electron-doped cuprates without the complications of structural and/or chemical disorder induced by chemical substitution in hole-doped materials. Recently, we discovered that when superconductivity first appears in one family of electron-doped superconductors, $Pr_{0.88}LaCe_{0.12}CuO_{4\pm\delta}$ (PLCCO), a commensurate quasi-2D SDW order is also induced,[35] and both coexist with the residual three-dimensional (3D) AF state.[36] The optimally doped SC PLCCO, on the other hand, has no static SDW or residual AF order,[34,36] analogous to hole-doped LSCO as depicted in Fig. 1.[6–9]

For prototypical electron-doped $Nd_{2-x}Ce_xCuO_4$ (NCCO),[30,31] previous neutron scattering experiments show a drastic suppression of the static 3D AF order when superconductivity is established.[37] However, the static AF order persists even for NCCO with optimal bulk superconductivity ($T_c=25$ K).[38] In the initial neutron scattering experiments on the slightly underdoped SC $Nd_{1.86}Ce_{0.14}CuO_4$, Matsuda *et al.*[39] found that a 10 T c-axis-aligned magnetic field has no effect on the residual AF order in the sample. On the other hand, we discovered that such fields enhance magnetic intensities at AF ordering positions in an optimally doped $Nd_{1.85}Ce_{0.15}CuO_4$.[40,41] The induced AF moments scale approximately linearly with the applied field, saturate at B_{c2}, and then decrease for higher fields. These results thus indicate that AF order is a competing ground state to superconductivity in electron-doped $Nd_{1.85}Ce_{0.15}CuO_4$.[42]

Although electron-doped NCCO offers a unique opportunity for studying the superconductivity-suppressed ground state of high-T_c cuprates, the system has one important complication. The as-grown material is NSC, and must be oxygen reduced to render the system superconducting. This reducing process has been found to produce a small quantity of the cubic $(Nd,Ce)_2O_3$ as an impurity phase.[41,43–46] Generally, a small amount (0.01% to 1%) of randomly distributed impurity would be unobservable, but $(Nd,Ce)_2O_3$ stabilizes as an oriented crystalline lattice in the NCCO matrix because its lattice constant is about $2\sqrt{2}$ larger than the planer lattice constant of the tetragonal NCCO ($a=3.945$Å and $a_{NO}=2\sqrt{2}a$). This in-plane lattice match with NCCO means reflections at $(H,K,0)$ of NCCO in reciprocal space may also stem from $(Nd,Ce)_2O_3$, thus giving structural impurity peaks that match some of the magnetic peaks [such as (0.5,0.5,0)]. In the paramagnetic state of $(Nd,Ce)_2O_3$, a field induces a net magnetization on Nd^{3+}, which can then contaminate the intensity of the cuprate magnetic peak such as (0.5,0.5,0).[41,43–46]

There are three ways to resolve this impurity problem and determine the intrinsic properties of electron-doped materials. First, since the impurity and cuprate peaks are not lattice matched along the c-axis direction (the lattice constant of impurity is about 10% smaller than that of NCCO), the impurity peaks occur at positions such as $(0.5,0.5,L)$ $L=2.2$, 4.4, and so on.[41,43] This allows the impurity scattering to be determined separately, and the in-plane scattering can then be corrected by subtracting the impurity contribution to ascertain the NCCO contribution of the in-plane peaks.[41,45]

Second, with a c-axis-aligned magnetic field and c axis in the scattering plane, the nonzero integer L positions ($L=1,2,3,$ …) can be measured without any possible impurity contribution. We carried out such an experiment using a horizontal field magnet and found that application of a 4 T c-axis-aligned magnetic field enhances the (0.5,0.5,3) AF reflection in the optimally doped SC $Nd_{1.85}Ce_{0.15}CuO_4$.[41] Both procedures show unambiguously that there is a field-induced moment in electron-doped $Nd_{1.85}Ce_{0.15}CuO_4$, whose behavior is similar to that observed in the hole-doped systems.

Although our previous experiments[40,41,45] have demonstrated the intrinsic nature of the field-induced effect in SC $Nd_{1.85}Ce_{0.15}CuO_4$, it is still interesting to perform field-induced experiments on samples free of Nd because application of a magnetic field is known to induce a large moment on rare-earth Nd^{3+} spins that may conceal the intrinsic field dependence of the Cu^{2+} moments. Electron-doped $Pr_{1-x}LaCe_xCuO_{4\pm\delta}$, where Pr^{3+} has a singlet ground state[47] and La is nonmagnetic, is ideal for this purpose. Using single crystals of $Pr_{1-x}LaCe_xCuO_{4\pm\delta}$ with $x=0.11$ ($T_c=16$ K) and $x=0.15$ ($T_c=26$ K), Fujita $et\ al.$[48] found that a c-axis-aligned magnetic field enhances the residual AF order in the $x=0.11$ sample at (0.5,1.5,0) position, but has no effect in the overdoped $x=0.15$ sample. The authors conclude that a c-axis field changes both the magnetic intensity and the onset of the Néel ordering temperature T_N for the $x=0.11$ sample, with the maximum field effect at ~5 T.[48]

Our approach to this problem has been slightly different from that of Fujita $et\ al.$[48] Instead of preparing different SC $Pr_{1-x}LaCe_xCuO_{4\pm\delta}$ samples as a function of Ce doping, we grew single crystals of PLCCO using a traveling solvent floating zone furnace. As-grown, PLCCO has a noncollinear Cu spin structure as shown in Fig. 2(a) with a small induced Pr moment due to Cu-Pr interaction.[49] When the AF ordered semiconducting PLCCO is transformed into a superconductor by annealing in pure Ar, the SC transition temperatures (T_c's) can be controlled by judicially tuning the annealing temperature.[34] This approach avoids complications of Ce substitution for different T_c materials. For underdoped samples with T_c's below 25 K, superconductivity coexists with both the 3D AF-type order of the undoped material and a commensurate quasi-2D SDW modulation.[36] Optimally doped PLCCO has no static SDW or residual AF order.

In this paper, we present comprehensive neutron scattering studies of four single crystals of n-type PLCCO from a semiconductor with $T_N=186$ K to superconductors with $T_c=16$ K, 21 K, and 24 K, respectively [Figs. 1(a) and 3(a)]. When a magnetic field is applied along the $[\bar{1},1,0]$ direction parallel to the CuO_2 plane, the noncollinear AF spin structure of PLCCO is transformed into a collinear one through a "spin-flop" transition.[49] Such a spin-flop transition is continuous in semiconducting PLCCO but gradually changes to discontinuous with increasing doping and the appearance of superconductivity. For SC PLCCO, an in-plane field only induces a spin-flop transition but does not change the effective Cu^{2+} or Pr^{3+} moments for fields up to 14 T. A c-axis-aligned magnetic field, on the other hand, enhances the quasi-2D SDW order at (0.5,0.5,0) for underdoped PLCCO, but has no effect on the 3D AF order in the NSC
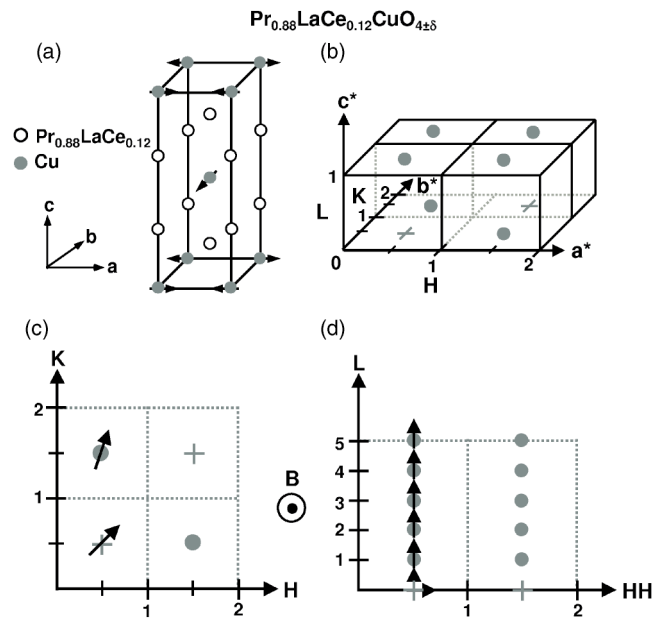

FIG. 2. (a) Schematic diagram of the noncollinear spin structure of PLCCO, (b) allowed AF Bragg peaks from the spin structure of (a), (c) reciprocal space probed in the $[H,K,0]$ scattering plane where the applied field is along the c axis. Solid circles are allowed AF Bragg peak positions in the $[H,K,0]$ plane. (d) Similar experiments in the $[H,H,L]$ zone where the field is along the $[\bar{1},1,0]$ direction in the CuO_2 plane. Arrows indicate the scan directions in our experiments.
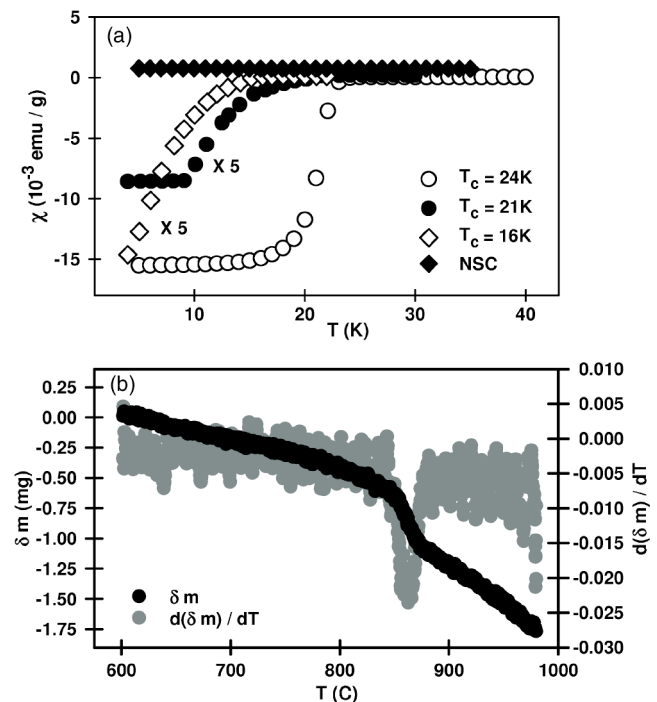

FIG. 3. (a) Magnetic susceptibility measurements of $Pr_{0.88}LaCe_{0.12}CuO_{4\pm\delta}$ single crystals under a small (5–10 G) field in the CuO_2 plane. (b) Temperature dependence of weight change and its derivative of a $Pr_{1.18}La_{0.7}Ce_{0.12}CuO_{4-\delta}$ in the annealing process.

and SC samples. Since the same 14 T field along the $[\bar{1},1,0]$ direction parallel to the CuO_2 plane has no effect on $(0.5, 0.5, 0)$ and on the lattice Bragg peaks of the $(Pr, La, Ce)_2O_3$ impurity phase, we conclude that the *c*-axis field-induced effect is intrinsic to PLCCO and arises from the suppression of superconductivity.

The rest of the paper is organized as follows: in Sec. II we describe the details of sample preparation methods and neutron-scattering experimental setup. The main experimental results are summarized in Sec. III, where Sec. III A reviews the zero-field magnetic properties, Sec. III B discusses the effects of in-plane magnetic fields on the AF spin structure, Sec. III C summarizes the magnetic field effect on the NSC PLCCO and impurity $(Pr, La, Ce)_2O_3$ phase, Sec. III D presents the comprehensive *c*-axis field effect studies and their temperature dependence for different SC PLCCO samples, and finally Sec. III E discuss the anisotropy of the field effect by comparing the in-plane and *c*-axis field effect on the $T_c = 21$ K SC sample. In Sec. IV, we compare our results with previous experiments in *p*- and *n*-type materials. A brief summary is given in Sec. V.

II. EXPERIMENTAL DETAILS

We grew high quality PLCCO single crystals (cylindrical rods weight 0.8–1.5 grams with mosaicity $<1°$) using the traveling solvent floating zone technique and annealed the samples in pure Ar at different temperatures to control the SC transition temperatures. The partial substitution of Pr with La was used to stabilize the crystal growth without introducing significant lattice distortions.[50] We obtained three SC PLCCO samples with the onset temperature for bulk superconductivity at $T_c = 24$ K, 21 K, and 16 K from magnetic susceptibility measurements [Fig. 3(a)]. The $T_c = 24$ K and 21 K samples are obtained by annealing the as-grown single crystals in pure argon at 970 °C and 940 °C for 24 hours, respectively. To obtain the $T_c = 16$ K crystal, the as-grown sample was annealed in pure argon at 915 °C for 1 week. The SC PLCCO of $T_c = 21$ K and 16 K are near the phase boundary between AF and SC phases and the $T_c = 24$ K sample is in the optimally doped regime. We also obtained a NSC sample by annealing one of the SC $T_c = 16$ K samples in air at 900 °C for 24 hours.[36]

One of the open questions in electron-doped superconductors is the role of the annealing process to superconductivity.[30] In earlier works, it was postulated that as-grown NSC samples have excess oxygen atoms above copper sites (apical oxygen). These extraneous oxygen atoms have been believed to induce a local disordered potential that localizes doped electrons and therefore prohibits superconductivity.[51] When the annealing process removes these defect oxygen atoms at apical sites, the electrons will not be localized and the superconductivity appears. The magnitude of the Hall coefficient in annealed NCCO ($x = 0.15$) decreases dramatically below $T < 100$ K, very differently from the as-grown sample.[51] This suggests that annealing changes the mobile charge density. To understand what annealing does to our PLCCO samples, we have performed thermogravimetric analysis (TGA) of our samples under dif-

ferent annealing conditions. Figure 3(b) shows the temperature dependence of the weight change for a $Pr_{1.18}La_{0.7}Ce_{0.12}CuO_{4\pm\delta}$ sample during the annealing process. The large drop in weight change shows up as a kink in the data and a sharp dip in its derivative; we interpret this kink to be indicative of the point where the oxygen content becomes the closest to stoichiometry, namely $\delta \simeq 0$.[50] In any case, the TGA data give the most direct evidence that oxygen content of the sample is reduced during the annealing process.

While TGA analysis indicates a decreased oxygen content after the reduction process, it is still unclear whether the apical oxygen is removed.[52,53] Indeed, recent Raman and crystal-field infrared transmission results suggest that instead of removing apical oxygen as originally thought, reduction of optimally doped $Pr_{2-x}Ce_xCuO_{4\pm\delta}$ and NCCO samples actually involves only oxygens in the CuO_2 plane.[54,55] Clearly, the exact oxygen content and their arrangements in the crystal before and after the reduction need to be sorted out by future studies.

Another issue to be noted regarding the PLCCO material is the relevance of the $(Pr, La, Ce)_2O_3$ impurity phase, which plays the same role in PLCCO as the $(Nd, Ce)_2O_3$ phase in NCCO. To understand the effect of annealing on this impurity phase, we have performed systematic synchrotron x-ray diffraction investigations on as-grown NSC, SC, and reoxygenated NSC PLCCO samples at the Advanced Photon Source, Argonne National Laboratory. We confirm that the $(Pr, La, Ce)_2O_3$ impurity phase can be produced by annealing and but it vanishes after the reoxygenation process;[33] such a behavior is rather strange, but is understandable if the host PLCCO crystals are slightly Cu deficient. To confirm this possibility, inductively coupled plasma atomic-emission spectroscopy (ICP-AES) analysis was performed on a batch of crystals that are nominally $Pr_{1.18}La_{0.7}Ce_{0.12}CuO_{4\pm\delta}$. The reference solution is prepared by diluting commercial standard solutions not by the volume but by the weight, which enables us to calculate the cation concentration of the reference with a high resolution. A piece of the $Pr_{1.18}La_{0.7}Ce_{0.12}CuO_{4\pm\delta}$ crystal (1 mg) is dissolved into a 30 cm^3 of HNO_3 (1 mol/liter). The analyzed cation ratio of the nominally $Pr_{1.18}La_{0.7}Ce_{0.12}CuO_{4\pm\delta}$ sample was Pr:La:Ce:Cu = 1.20:0.68:0.12:0.97, with a relative error of less than 1% for each element. This result shows that Cu is indeed deficient by about 3% in the $Pr_{1.2}La_{0.7}Ce_{0.12}CuO_{4\pm\delta}$ crystal, which is probably also true for PLCCO. Assuming that as-grown PLCCO samples are slightly Cu deficient as $Pr_{1.2}La_{0.7}Ce_{0.12}CuO_{4\pm\delta}$, the effect of annealing is then to remove oxygen in PLCCO to form the $(Pr, La, Ce)_2O_3$ impurity and make the remaining crystal structure more perfect for superconductivity. This analysis can potentially explain why the $(Pr, La, Ce)_2O_3$ impurity phase can be reversibly produced.[33]

Our neutron scattering measurements were performed on the HB-1A, HB-1, and HB-3 triple-axis spectrometers at the high-flux-isotope reactor (HFIR), Oak Ridge National Laboratory (ORNL) and on the E4 two-axis diffractometer and E1 triple-axis spectrometer at the Berlin Neutron Scattering Center, Hahn-Meitner-Institute (HMI). The field effect experiments on SC samples of $T_c = 24$ K, 21 K, and 16 K and

the NSC sample ($T_N = 186$ K) were carried out at HFIR using a 7 T vertical field SC magnet.[25] The collimations were 48″-40″-sample-40″-102″ (full-width at half-maximum) from the reactor to the detector and the final neutron energies were fixed at either $E_f = 14.6$ meV or 13.5 meV. For high magnetic field experiments, we used the VM-1 14.5 T vertical field SC magnet at HMI and a 40″-40″-sample-40″ collimation with a fixed neutron final energy of 13.6 meV. A pyrolytic graphite (PG) monochromator and PG analyzer were used and PG filters were placed in front of the sample to remove higher order contaminations from the incident beam. The samples were clamped on solid aluminum brackets similar to those used in the NCCO experiments.[41] However, a c-axis-aligned field almost exerts no torque on PLCCO because of the non-magnetic singlet nature of the Pr ground state.

We use elastic neutron scattering to probe AF order and label the momentum transfer $\mathbf{Q} = (q_x, q_y, q_z)$ in Å^{-1} as $(H, K, L) = (q_x a / 2\pi, q_y b / 2\pi, q_z c / 2\pi)$ in the reciprocal lattice units (r.l.u.) appropriate for the tetragonal unit cell of PLCCO (space group $I4/mmm$, $a = b = 3.98$ and $c = 12.27$ Å). Here a and c are in-plane and out-of-plane lattice constants, respectively. The crystals were aligned in two different geometries, $[H, K, 0]$ and $[H, H, L]$ scattering planes. The vertical magnetic field was applied along the c axis in the former scattering plane and was applied along the $[\bar{1}, 1, 0]$ direction ($\mathbf{B} \parallel ab$-plane) in the latter case. The $[H, H, L]$ geometry was also used to search for quasi-2D SDW order at zero-field using a two-axis energy integrated mode [Fig. 2(d)], to determine the field-induced effect on the impurity phase, and investigate the field-induced spin-flop transitions. In the $[H, K, 0]$ geometry, we studied the c-axis field-induced effect on SC and NSC PLCCO. The anisotropy of the field-induced effect can be determined by comparing the results in these two geometries since the magnetic field along the c axis suppresses the SC much more strongly than that for the same field in the ab plane.

III. RESULTS

A. Magnetic properties of superconducting and nonsuperconducting Pr$_{0.88}$LaCe$_{0.12}$CuO$_{4 \pm \delta}$ at zero field

To determine the influence of a magnetic field on the AF order of PLCCO, it is helpful to know the magnetic structure of its parent compound. Pr$_2$CuO$_4$ has a body-centered tetragonal structure with space group $I4/mmm$.[56] The spins of Cu^{2+} ions have AF ordering in the CuO$_2$ plane due to strong in-plane exchange interaction. The orientation of spins in adjacent planes is noncollinear governed by the weak pseudodipolar interaction between planes, since exchange field on each copper ion by neighboring planes is canceled due to body-centered tetragonal crystal symmetry.[56] The spins at $(0,0,0)$ and $(0.5,0.5,0.5)$ positions are along the $[1,0,0]$ and $[0,\bar{1},0]$ directions, respectively [Fig. 2(a)]. In this magnetic structure, the AF Bragg peak at $(0.5,0.5,0)$ is disallowed. The allowed magnetic Bragg peaks are at $(0.5,0.5,L)$ ($L = 1,2,3,...$) and $(0.5,1.5,L)$ ($L = 0,1,2,3,...$) marked as solid dots in Fig. 2(b).
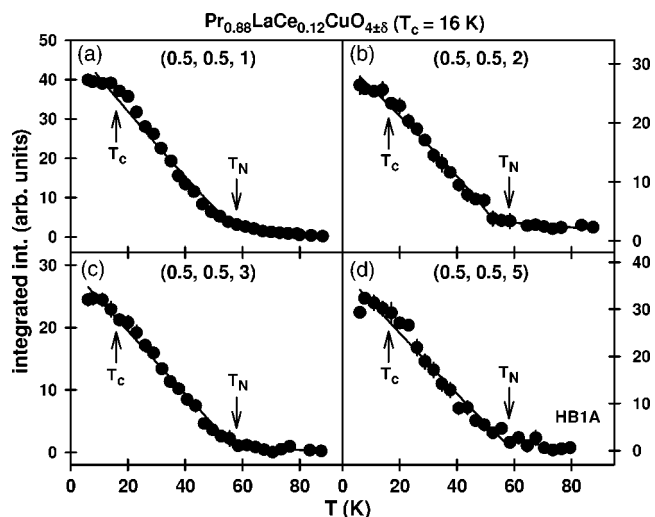

FIG. 4. Temperature dependence of integrated intensities at $(0.5, 0.5, L)$ for the $T_c = 16$ K PLCCO. The solid lines are guides to the eye. The arrows indicate T_c and T_N, respectively.

We performed neutron diffraction measurements at zero field on magnetic Bragg peaks $(0.5, 0.5, L)$ ($L = 1, 2, 3, 5$) to determine the magnetic structure of the superconducting $T_c = 16$ K PLCCO (Fig. 4). In principle, one cannot uniquely determine the spin structure of PLCCO based on magnetic intensities at $(0.5, 0.5, L)$ alone. However, since the spin structure of Pr$_{2-x}$Ce$_x$CuO$_4$ at all Ce doping levels is noncollinear as depicted in Fig. 2(a),[56] one would expect a similar magnetic structure in PLCCO because substitution of La^{3+} for Pr^{3+} will weaken the pseudodipolar interactions but not eliminate it. The integrated intensity comparison of $(0.5, 0.5, L)$ peaks to the calculated intensities confirms that the superconducting sample has the same noncollinear spin structure as that of the parent Pr$_2$CuO$_4$.

To estimate the effective Cu^{2+} and Pr^{3+} moments, we measured the temperature dependence of $(0.5, 0.5, L)$ reflections. By comparing the magnetic structure factor calculations (Table I) with that of the weak nuclear Bragg peak $(1,1,0)$, we calculate an ordered Cu^{2+} moment of $0.06 \pm 0.01 \mu_B$ at 5 K with negligible induced moment on Pr^{3+} ions for the $T_c = 16$ K PLCCO.[57] Since the induced Pr^{3+} moment contributes positively to the intensity of $(0.5, 0.5, 1)$ and $(0.5, 0.5, 2)$, but negatively to $(0.5, 0.5, 3)$, the temperature dependent measurements of $(0.5, 0.5, L)$ should reveal deviations from power law fits when the Pr-induced moment becomes significant.[49] In addition, the $(0.5, 0.5, 5)$ peak should exhibit only the temperature dependence of the Cu^{2+} moment as there are essentially no Pr^{3+} moment contributions to this reflection (Table I). Since all magnetic peaks at $(0.5, 0.5, L)$ show a similar temperature dependence as $(0.5, 0.5, 5)$ (Fig. 4), we conclude that there is negligible Pr-induced moment above 4 K in the $T_c = 16$ K PLCCO.

In a recent work, we have systematically investigated how superconductivity develops from the AF ordered insulating state in PLCCO.[36] By carefully tuning the annealing temperature of as-grown NSC PLCCO, we can control the strength of the AF order and superconductivity without additional complications such as disorder associated with con-

TABLE I. Magnetic structure factor calculations for noncollinear $(F_{nc})^2$ and collinear $(F_c)^2$ spin structures as seen in Figs. 7(a) and 7(b). Here $\gamma e^2/(2mc^2) = 0.2695 \times 10^{-12}$ cm, $f_{cu,pr}$, $M_{cu,pr}$ are magnetic form factors and ordered magnetic moments for Cu^{2+} and Pr^{3+} ions, respectively.

(H,K,L)	$(F_{nc})^2$
(0.5,0.5,0)	0
(0.5,0.5,1)	$32.0(\gamma e^2/2mc^2)^2(f_{cu}M_{cu}+0.5310f_{pr}M_{pr})^2$
(0.5,0.5,2)	$14.6(\gamma e^2/2mc^2)^2(f_{cu}M_{cu}+0.2391f_{pr}M_{pr})^2$
(0.5,0.5,3)	$32.0(\gamma e^2/2mc^2)^2(f_{cu}M_{cu}-0.8196f_{pr}M_{pr})^2$
(0.5,0.5,4)	$24.6(\gamma e^2/2mc^2)^2(f_{cu}M_{cu}+0.7500f_{pr}M_{pr})^2$
(0.5,0.5,5)	$32.0(\gamma e^2/2mc^2)^2(f_{cu}M_{cu}-0.0856f_{pr}M_{pr})^2$

| (H,K,L)	$(F_c)^2$
(0.5,0.5,0)	0
(0.5,0.5,1)	0
(0.5,0.5,2)	$29.2(\gamma e^2/2mc^2)^2(f_{cu}M_{cu}+0.2391f_{pr}M_{pr})^2$
(0.5,0.5,3)	0
(0.5,0.5,4)	$49.2(\gamma e^2/2mc^2)^2(f_{cu}M_{cu}+0.7500f_{pr}M_{pr})^2$
(0.5,0.5,5)	0

FIG. 5. **Q** scans in the $[H,K,0]$ zone at low and high temperatures for different PLCCO samples. (a)–(d) Scans along the $[H,H,0]$ direction around (0.5,0.5,0) for $T_c = 24$ K, 21 K, 16 K, and NSC PLCCO. (e)–(h) Similar scans along the $[H,3H,0]$ direction around (0.5,1.5,0). This figure is reproduced from Fig. 2 of Ref. 36.

ventional chemical substitution. The temperature dependence of (0.5,1.5,0) shows that the Néel temperature T_N decreases linearly with increasing T_c, and becomes zero at the maximum T_c of 24 K. Although the commensurate AF position (0.5,0.5,0) is forbidden in the noncollinear spin structure of PLCCO [Fig. 2(a)], clear magnetic scattering is observed at (0.5,0.5,0) in underdoped SC PLCCO ($T_c = 21$ K and 16 K) in the $[H,K,0]$ scattering geometry (Fig. 5). This magnetic component is on top of the structural superlattice peak resulting from the annealing process.[33] Solid lines in Fig. 5 are Gaussian fits to the peaks on sloping backgrounds, where $I = bkgd + I_0 \exp[-(H-H_0)^2/(2\sigma^2)]$. Fourier transform of the Gaussian peaks give a minimum in-plane coherence length (CL) of ~200 Å for all four samples using $CL = [\sqrt{\ln(2)}/\pi](a/\sigma)$ for $[H,H,0]$ scans and $CL = [\sqrt{\ln(2)/5}/\pi](a/\sigma)$ for $[H,3H,0]$ scans. To determine the c-axis correlations of the magnetic scattering at (0.5,0.5,0), we aligned the crystal in the $[H,H,L]$ scattering plane but found no large intensity gain centered at $L=0$ in $[0.5,0.5,L]$ scans.[36]

If underdoped PLCCO has a quasi-2D SDW with strong correlation in the CuO_2 plane but weak coupling along the c axis, the coarse vertical resolution of the triple-axis spectrometer will integrate a much larger region of the c-axis magnetic rod in the $[H,K,0]$ plane than that in the $[H,H,L]$ zone. As a consequence, the quasi-2D scattering should be more easily observable in the $[H,K,0]$ zone. The presence of a quasi-2D SDW can be tested using the 2-axis energy integrated mode by aligning the outgoing wave vector k_f parallel to the 2D rod direction (c axis) [Fig. 4(d) in Ref. 36]. The temperature dependent scattering around $(0.5,0.5,L)$ in underdoped PLCCO ($T_c = 21$ and 16 K) suggests the presence of quasi-2D SDW modulation [Figs. 6(c) and 6(d)].[36] Because these data were collected using the 2-axis mode, which integrates elastic, inelastic magnetic scattering as well as
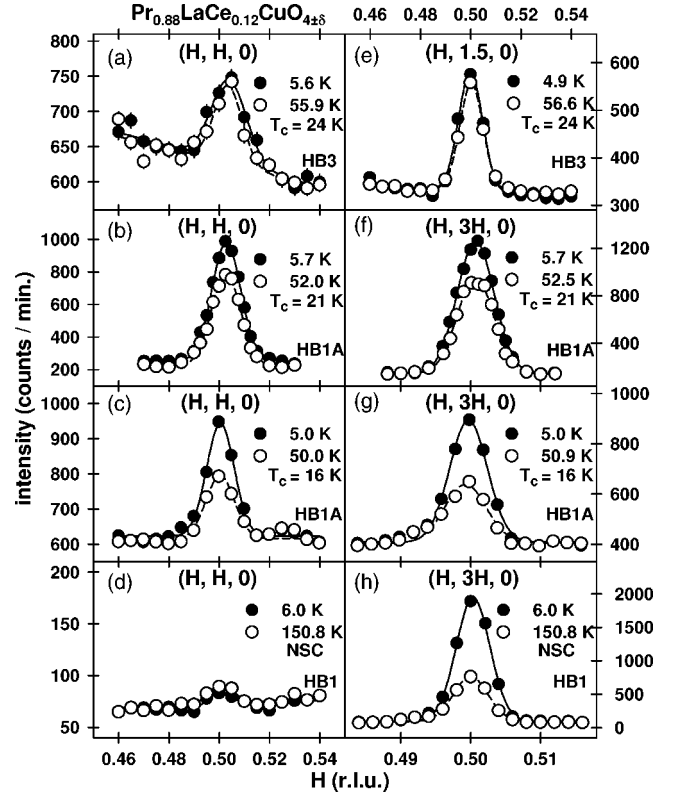
phonons, its temperature dependence is not a reliable measure of the quasielastic diffusive magnetic scattering in Fig. 3 of Ref. 36. For optimally doped PLCCO ($T_c = 24$ K), there is no evidence for the SDW or 3D AF order as shown by the temperature independent scattering at (0.5,0.5,0) and (0.5,1.5,0) [Figs. 5(a), 5(e), 6(a), and 6(b)]. For NSC PLCCO, the scattering only shows the static 3D AF order with a small Pr-induced moment at low temperatures.[36]

B. Spin-flop transition on superconducting and nonsuperconducting $Pr_{0.88}LaCe_{0.12}CuO_{4\pm\delta}$

A magnetic field applied in the $[\bar{1},1,0]$ direction of the CuO_2 planes induces a spin-flop transition from noncollinear to collinear spin structure in electron-doped parent compounds Nd_2CuO_4 and Pr_2CuO_4 (Fig. 7).[58,59] For lightly electron-doped $Pr_{1.29}La_{0.7}Ce_{0.01}CuO_{4\pm\delta}$, Lavrov *et al.* discovered that the spin-flop transition is intimately related to the magnetoresistance effect.[49] Similar spin-charge coupling was also found in a separate study on lightly doped $Nd_{1.975}Ce_{0.025}CuO_4$.[60] The critical field for the transition from a noncollinear spin structure to a collinear one increases with decreasing temperature. For lightly electron-doped $Pr_{1.29}La_{0.7}Ce_{0.01}CuO_{4\pm\delta}$, the critical field increases from 0.5 T at 150 K to 2 T at 5 K.[49]

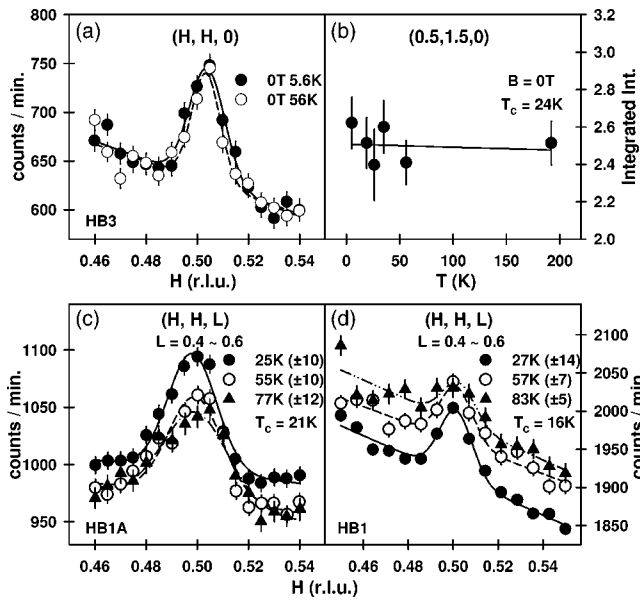We systematically investigated the effect of an in-plane magnetic field on the spin structure of PLCCO because su-

FIG. 6. (a) $[H,H,0]$ scans around $(0.5,0.5,0)$ at 5.6 K and 56 K for the optimally doped $T_c=24$ K PLCCO. The observed peak at $(0.5,0.5,0)$ has nonmagnetic origin. (b) The temperature dependence of the integrated intensities at $(0.5,1.5,0)$ for the $T_c=24$ K PLCCO. There is no evidence for static SDW and/or AF orders in the optimally doped PLCCO. (c) and (d) Two-axis mode scans along the $[H,H,0]$ direction around $(0.5,0.5,L)$ $(0.4<L<0.6)$ at different temperatures for underdoped SC $T_c=21$ K and 16 K PLCCO, respectively. Magnetic scattering clearly decreases with increasing temperature for both compounds.

perconductivity is not much affected in this geometry. The magnetic structure factors at $(0.5,0.5,L)$ for the noncollinear and collinear phases of PLCCO are summarized in Table I. In the collinear spin structure, the magnetic peaks are disallowed at $(0.5,0.5,L)$ with $L=$odd integer. We probed the $(0.5,0.5,1)$ and $(0.5,0.5,2)$ magnetic peaks as a function of the field at low temperature. Figure 8 summarizes the effect of a $\mathbf{B} \| [\bar{1},1,0]$ field on the $(0.5,0.5,1)$ and $(0.5,0.5,2)$ magnetic peaks in different samples of PLCCO at 5 K. The solid lines are Gaussian fits to the data. The c-axis coherence lengths are resolution limited and about 660 Å for all three samples estimated using $\mathrm{CL}=[\sqrt{2\ln(2)}/\pi](c/\sigma)$. Therefore, the residual AF order at $(0.5,0.5,L)$ $(L=1,2,\ldots)$ in underdoped and NSC PLCCO are 3D and different from the quasi-2D diffusive scattering at $(0.5,0.5,0)$.
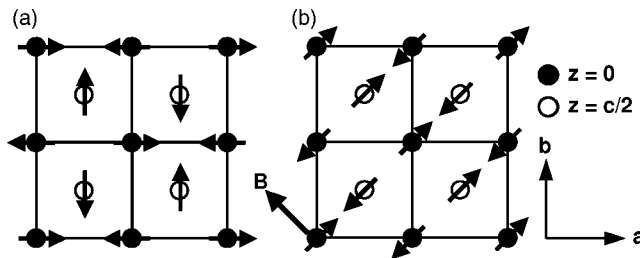

FIG. 7. Magnetic structures of Cu^{2+} ions in PLCCO. (a) Noncollinear structure at zero field. (b) Collinear structure transformed by a magnetic field applied along the $[\bar{1},1,0]$ direction.
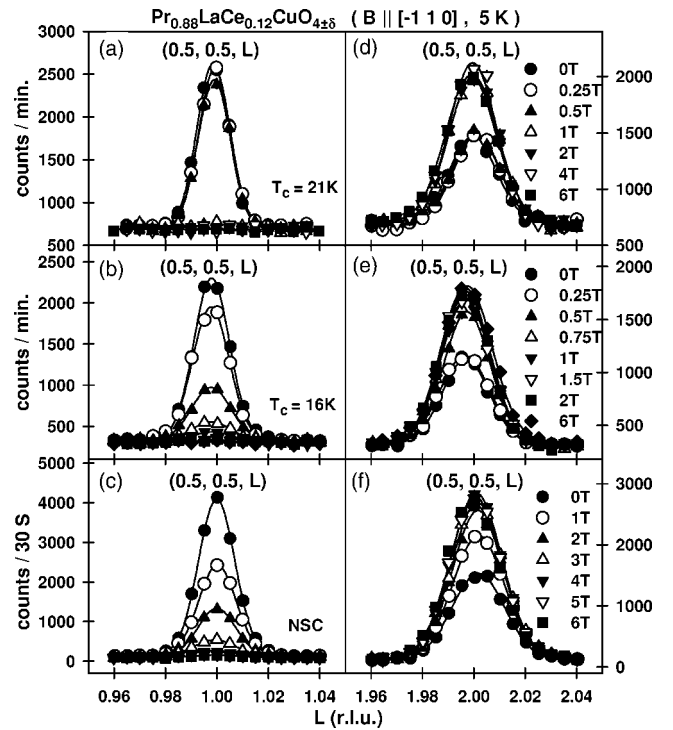

FIG. 8. Magnetic field dependence of the scattering around $(0.5,0.5,L)$ at 5 K, a temperature well below the perspective T_N's for various SC and NSC PLCCO samples. (a)–(c) L scans around $(0.5,0.5,1)$, (d)–(f) L scans around $(0.5,0.5,2)$ for $T_c=21$ K, 16 K and NSC PLCCO samples. The $T_c=21$ K sample shows an abrupt spin-flop transition and the $T_c=16$ K and the NSC samples display a more gradual spin-flop transition. The solid lines are Gaussian fits to the data.

For the $T_c=21$ K PLCCO, a 1 T applied field diminishes the $(0.5,0.5,1)$ and enhances the $(0.5,0.5,2)$ magnetic reflections, thus indicating that the magnetic structure has been transformed from the noncollinear to collinear structure by the field [Figs. 7(a), 7(b), 8(a), and 8(d)]. This sharp transition in the $T_c=21$ K PLCCO is surprising because spin-flop transitions for $\mathbf{B}\|[\bar{1},1,0]$ fields in lightly doped $Pr_{1.29}La_{0.7}Ce_{0.01}CuO_{4+\delta}$,[49] $Nd_{1.975}Ce_{0.025}CuO_4$,[60] Nd_2CuO_4,[58] and Pr_2CuO_4 (Ref. 56) are more gradual and continuous.

To understand the evolution of such behavior as PLCCO is transformed from a superconductor to an antiferromagnet, we performed similar measurements on the $T_c=16$ K and the NSC PLCCO. The outcome [Figs. 8(b), 8(c), 8(e), and 8(f)] suggests that spin-flop transitions become sharper as superconductivity is developed with increasing T_c and decreasing T_N. Figure 9 summarizes the integrated intensities of $(0.5,0.5,1)$ and $(0.5,0.5,2)$ as a function of increasing field for the three PLCCO samples at 5 K. The inset in Fig. 9(b) shows that a higher Néel temperature T_N requires a larger critical field $\mathbf{B}_{sp}$ for the spin-flop transition. $\mathbf{B}_{sp}$ therefore decreases with decreasing T_N and reducing Cu moment.

From the magnetic structure factor calculations in Table I, we find that the ratio of integrated intensities of $(0.5,0.5,L =$even) at collinear and noncollinear states is $[F_c(0.5,0.5,L =$even$)/F_{nc}(0.5,0.5,L=$even$)]^2=2$ if the Pr and Cu moments under field are the same as that at zero field. Inspection of
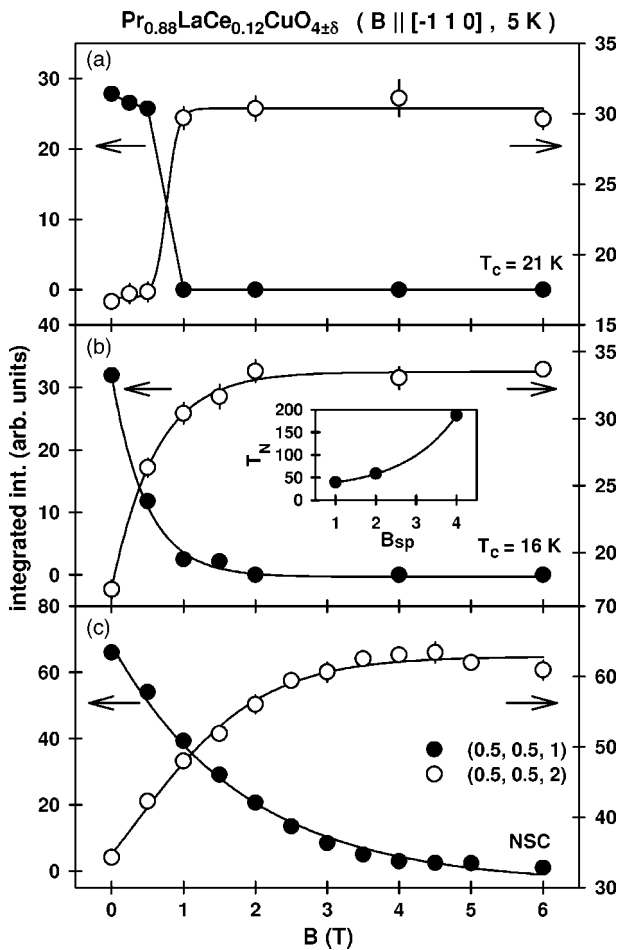
FIG. 9. Integrated intensities of $(0.5, 0.5, L)$ as a function of a magnetic field for (a) $T_c = 21$ K, (b) $T_c = 16$ K, (c) NSC samples at 5 K. The inset in (b) shows that the sample with higher Néel temperature requires a higher critical field to induce the spin-flop transition.

Figs. 8 and 9 for $(0.5, 0.5, 2)$ shows that this is indeed the case. Therefore, a moderate magnetic field ($\leqslant 6$ T) that causes the spin-flop transition does not induce additional moments on Cu or Pr sites in PLCCO.

To further determine the effect of a magnetic field on Pr/Cu moments after the spin-flop transition, we measure the temperature dependence of the scattering at $(0.5, 0.5, L)$ ($L = 2, 4, 6$) for fields just above $\mathbf{B}_{sp}$ and at 6 T. This comparison allows us to determine whether application of additional field induces Cu/Pr moments in the collinear state of PLCCO after the spin-flop transition. Inspection of the data in Fig. 10 reveals no appreciable difference between 1.5 T and 6 T in the temperature range probed, consistent with the notion that a 6 T in-plane field does not induce additional Cu/Pr moments for the $T_c = 16$ K PLCCO.

To see if a larger in-plane field will affect the Cu/Pr moment, we measured the field-dependence of the $(0.5, 0.5, 2)$ and $(0.5, 0.5, 4)$ reflections up to 14 T for the $T_c = 21$ K PLCCO at HMI. The outcome, shown in Figs. 11(c)–11(e), clearly indicates that while a 1 T in-plane field enhances the intensity of the $(0.5, 0.5, 2)$ peak from that at zero field as expected from the spin-flop transition, further increasing the applied field to 14 T does not induce additional changes in
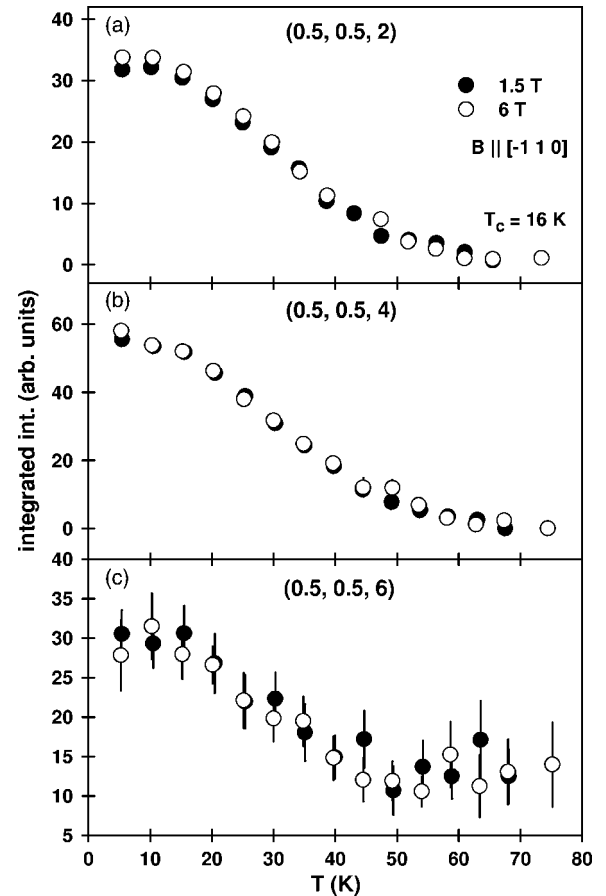

FIG. 10. The temperature dependence of the integrated magnetic Bragg intensities for $(0.5, 0.5, L)$ with $L = 2, 4, 6$ at 1.5 T and 6 T for the $T_c = 16$ K PLCCO. The spin-flop transition should have occurred above 1.5 T [see Fig. 9(b)]. The negligible changes of the integrated intensities indicate that an in-plane magnetic field of 6 T does not affect the Cu and Pr moment. It only transforms the magnetic structure from a noncollinear to a collinear one (Fig. 7).

the integrated intensity of the $(0.5, 0.5, 2)$ peak [Fig. 11(c)]. Therefore, a 14 T field does not alter the Cu/Pr moments within the uncertainty of our measurements. This is quite different from the effect of an in-plane field on $Nd_{1.85}Ce_{0.15}CuO_4$, where the $(0.5, 0.5, 2)$ reflection shows no intensity differences and the $(0.5, 0.5, 4)$ intensity decreases under a 7 T field [Figs. 11(a) and 11(b)].[40] For $Nd_{1.85}Ce_{0.15}CuO_4$, a 7 T $\mathbf{B} \| [\bar{1}, 1, 0]$ magnetic field not only causes a spin-flop transition but also induces magnetic moments on the Nd sites. The significant intensity drop at $(0.5, 0.5, 4)$ under 7 T arises because of the larger Nd moment contribution to the magnetic structure factor (Table I, for NCCO the Nd moment has opposite direction to Pr moment). Since PLCCO has negligible field-induced moment contribution from Pr, field-induced effects here should reveal the inherent Cu^{2+} spin correlations.

C. Magnetic field effect on the nonsuperconducting $Pr_{0.88}LaCe_{0.12}CuO_{4\pm\delta}$ and the cubic $(Pr,La,Ce)_2O_3$ impurity phase

Since the discovery of a c-axis magnetic field-induced effect in $Nd_{1.85}Ce_{0.15}CuO_4$,[40] there has been much debate
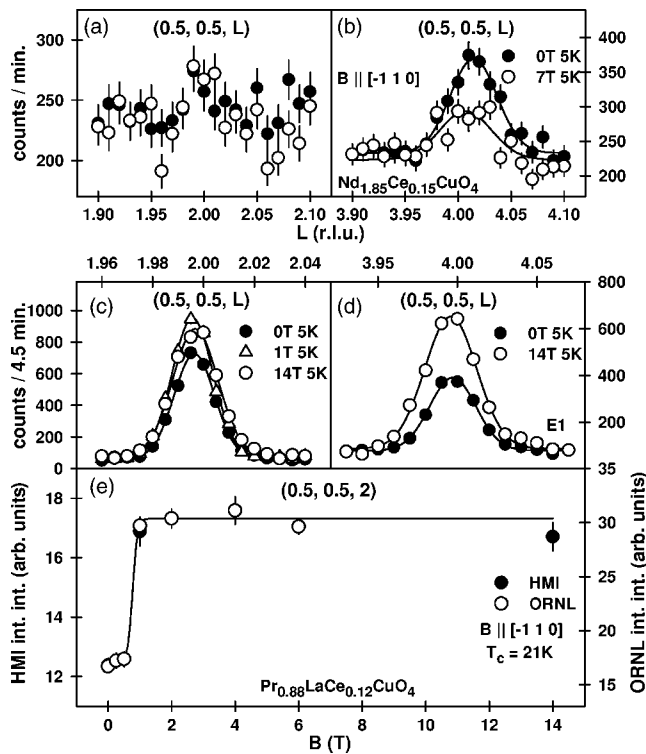
FIG. 11. The comparison of the influence of an in-plane field on the magnetic Bragg peaks of PLCCO and NCCO. (a) and (b) Low-temperature L scans across the magnetic peaks at $(0.5,0.5,2)$ and $(0.5,0.5,4)$ in NCCO (from Ref. 40). (c) and (d) Similar L scans across $(0.5,0.5,2)$ and $(0.5,0.5,4)$ in PLCCO. The intensity differences between NCCO and PLCCO is due the induced moment on Nd^{3+} in NCCO. (e) Integrated intensity of $(0.5,0.5,2)$ as a function of a field. Right after spin-flop transition, the integrated intensity shows no field dependence up to 14 T. This confirms that Pr moment is not induced by a field up to 14 T.

concerning the origin of the field-induced effect. While we argue that the observed effects are partially intrinsic to $Nd_{1.85}Ce_{0.15}CuO_4$,[41,44,45] Mang et al.[43,46] suggest that all the observed field-induced effect in Ref. 40 can be explained by paramagnetic scattering from the impurity $(Nd,Ce)_2O_3$ phase. Since there will always be paramagnetic scattering from $(Nd,Ce)_2O_3$ under the influence of a magnetic field in SC NCCO, it is more productive to study n-type superconductors where the impurity phase has no field-induced effect. SC PLCCO is a good candidate because Pr^{3+} in the impurity phase $(Pr,La,Ce)_2O_3$ has a nonmagnetic singlet ground state. To reveal the intrinsic magnetic field effect on Cu^{2+} magnetism in SC PLCCO, one must understand the field-induced effect on AF order in NSC PLCCO and impurity $(Pr,La,Ce)_2O_3$.

To determine the effect of a c-axis-aligned magnetic field on the AF order of NSC PLCCO, we use the reoxygenated sample ($T_N=186$ K) aligned in the $[H,K,0]$ scattering plane. Figures 12(a) and 12(b) show radial scans across $(0.5, -0.5,0)$ and $(0.5,-1.5,0)$ at zero and 6 T c-axis-aligned fields. To within the error of the measurements, a magnetic field of 6 T has no effect on either peak at 5 K although there are small differences in the background scattering of Fig.
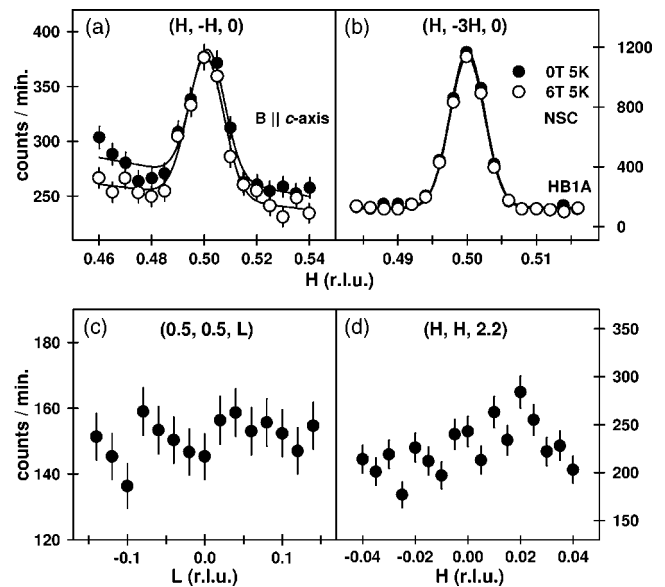

FIG. 12. (a) and (b) Magnetic field dependent scattering around $(0.5,-0.5,0)$ and $(0.5,-1.5,0)$ of NSC PLCCO in the $[H,K,0]$ scattering plane. Radial scans across (a) $(0.5,-0.5,0)$ and (b) $(0.5,-1.5,0)$ at 5 K with zero and 6 T fields, respectively. The magnetic field is applied along the c axis. While the scattering at $(0.5,-1.5,0)$ is mostly magnetic from the noncollinear AF order [Fig. 2(a)], the peak at $(0.5,-0.5,0)$ does not arise from $(Pr,La,Ce)_2O_3$ but is diffusive structural scattering of PLCCO similar to those seen in the SC $Nd_{1.85}Ce_{0.15}CuO_4$ (Ref. 41). This conclusion is confirmed by (c) $[0.5,0.5,L]$ and (d) $[H,H,2.2]$ scans across the impurity positions of NSC PLCCO in the $[H,H,L]$ scattering plane.

12(a) under field with unknown origin. Since a 6 T field along the c axis has no effect on NSC $Nd_{1.85}Ce_{0.15}CuO_4$,[41] we conclude that such field does not affect the AF structure or induce moments in NSC PLCCO or $Nd_{1.85}Ce_{0.15}CuO_4$.

Next, we consider the influence of a magnetic field on the impurity $(Pr,La,Ce)_2O_3$ phase. To separate the impurity phase from PLCCO, we aligned the SC PLCCO single crystals in the $[H,H,L]$ zone and applied a magnetic field along the $[\bar{1},1,0]$ direction.[41,46] Since $(Pr,La,Ce)_2O_3$ has essentially a cubic crystal structure with lattice parameter $\sim10\%$ smaller than the c-axis lattice parameter of PLCCO, one can probe the paramagnetic scattering from the impurity phase by simply looking around the $(0,0,2.2)$ position of PLCCO in the $[H,H,L]$ geometry.[41,46] Here, cubic reflections $(2,0,0)_c$ and $(0,0,2)_c$ from $(Pr,La,Ce)_2O_3$ can be indexed as $(0.5,0.5,0)$ and $(0,0,2.2)$ in PLCCO Miller indices, respectively. A $\mathbf{B}\|[\bar{1},1,0]$ field in the CuO_2 plane is along the $[1,0,0]$ direction of the cubic $(Pr,La,Ce)_2O_3$, equivalent to a c-axis-aligned field in PLCCO which is along the $[0,0,1]$ direction of $(Pr,La,Ce)_2O_3$.

The field effect on the $(Pr,La,Ce)_2O_3$ impurity phase was measured in optimally doped and underdoped SC PLCCO samples with $T_c=24$ K, 21 K, and 16 K. Following previous work on NCCO,[41,43,46] we probe the impurity peak positions $(0,0,2)_c$, $(1,1,0)_c$, and $(0,0,4)_c$ which correspond to PLCCO Miller indices $(0,0,2.2)/(0.5,0.5,0)$, $(0.5,0,0)$, and
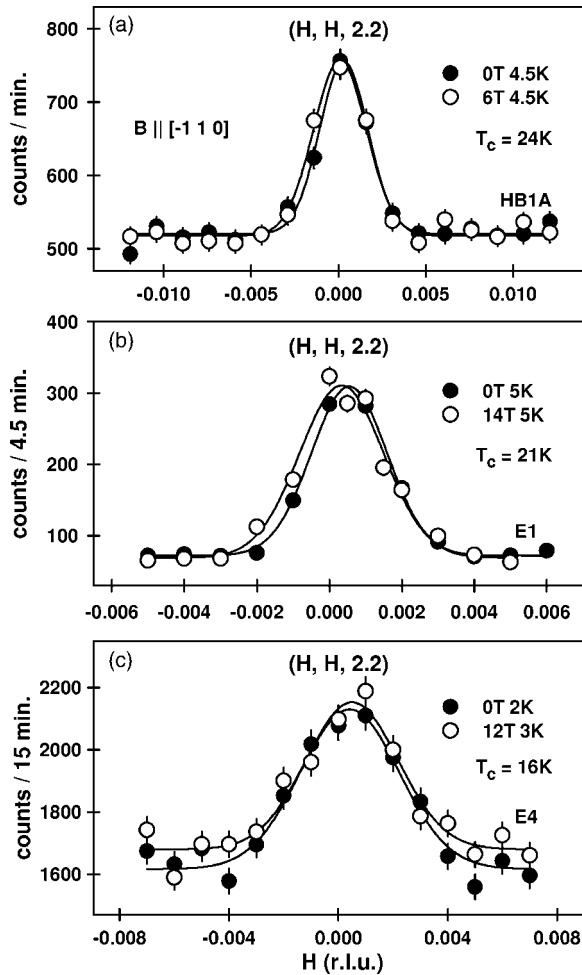
FIG. 13. Magnetic field effect on the impurity peak position $(0,0,2.2)$ at low temperatures. (a)–(c) Scans along the $[H,H,2.2]$ direction for the $T_c=24$ K, 21 K, and 16 K PLCCO, respectively. The magnetic fields are applied along the $[\bar{1},1,0]$ direction, similar to previous work on SC NCCO (Refs. 41 and 43).
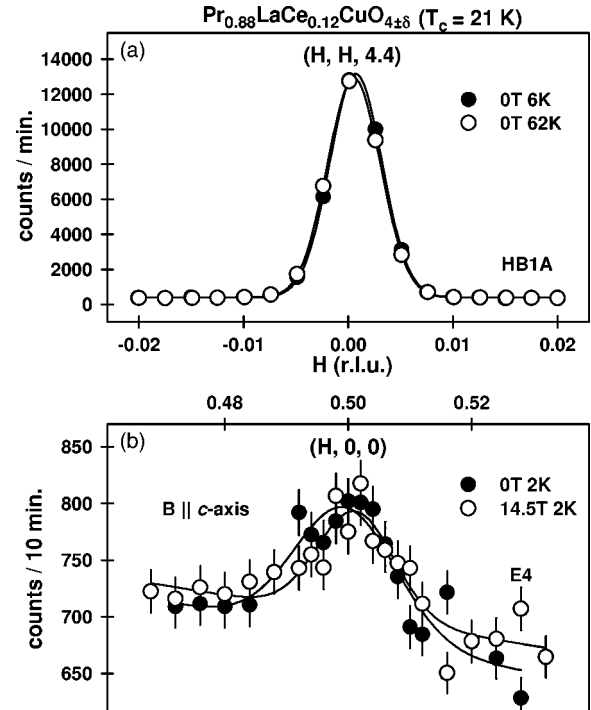

FIG. 14. (a) $[H,H,4.4]$ scan through $(0,0,4.4)$ position for impurity peak $(0,0,4)_c$ at low and high temperatures. The temperature independent scattering indicates that the impurity peak has no magnetic component. (b) Radial $[H,0,0]$ scan across $(0.5,0,0)$ of the impurity peak $(1,1,0)_c$ at zero and 14.5 T c-axis-aligned fields (Ref. 45). It shows no field-induced effect, indicating that the impurity phase cannot be polarized by a 14.5 T field.

$(0,0,4.4)$, respectively. Figure 13 summarizes the outcome around $(0,0,2.2)$ for the three SC PLCCO samples investigated. The $[H,H,2.2]$ scans across the impurity position at $(0,0,2.2)$ show no observable field-induced effect on the impurity phase up to 14 T [Figs. 13(a)–13(c)]. Additional measurements of the temperature dependent scattering around $(0,0,4.4)$ [Fig. 14(a)] and the c-axis field-dependent scattering around $(0.5,0,0)$ [Fig. 14(b)] on the $T_c=21$ K sample confirm that Pr^{3+} ions in $(Pr,La,Ce)_2O_3$ have a nonmagnetic singlet ground state and cannot be polarized by a 14.5 T field. In contrast, Nd^{3+} ions in the $(Nd,Ce)_2O_3$ impurity phase can be easily polarized by an applied field. Therefore, we can avoid the complication of field-induced paramagnetism from the impurity phase by studying PLCCO and the outcome should unambiguously reveal the intrinsic properties of Cu^{2+} magnetism in SC electron-doped materials.

D. Effect of a c-axis-aligned magnetic field on SDW and AF orders in superconducting $Pr_{0.88}LaCe_{0.12}CuO_{4\pm\delta}$

In this section, we describe the effect of a c-axis-aligned magnetic field on SC PLCCO samples. Since the preceding

section confirmed that the $(Pr,La,Ce)_2O_3$ impurity phase does not respond to an applied magnetic field, any field-induced effect on SC samples must be intrinsic to PLCCO. For the experiment, we aligned crystals in the $[H,K,0]$ scattering plane and applied magnetic fields along the c axis. Figure 15 shows the radial $[H,H,0]$ and $[H,3H,0]$ scans around $(0.5,0.5,0)$ and $(0.5,1.5,0)$ positions, respectively, for the SC $T_c=24$ K, 21 K, and 16 K samples. In all cases, we carefully applied the magnetic field above T_c and field cooled the samples to below T_c. For optimally doped PLCCO ($T_c=24$ K), a magnetic field of 6.5 T at 4.5 K does not affect the scattering at $(0.5,0.5,0)$ and $(0.5,1.5,0)$ [Figs. 15(a) and 15(e)], consistent with an earlier report on an overdoped PLCCO ($T_c=16$ K).[48] Note that in this case the peaks at both positions arise mostly from superlattice and $(Pr,La,Ce)_2O_3$ and there are no static AF orders in the sample [Figs. 6(a) and 6(b)].[36]

Underdoped SC samples ($T_c=21$ K and 16 K), however, show clear low-temperature field-induced intensity gain at the diffusive SDW position $(0.5,0.5,0)$ [Figs. 15(b)–15(d)], but not at the 3D AF ordered position $(0.5,1.5,0)$ [Figs. 15(f)–15(h)]. In particular, the field-induced intensity appears to increase with increasing magnetic field for the $T_c=21$ K PLCCO [Figs. 15(b) and 15(c)]. On warming to temperatures above T_c but below T_N, the field-induced effect becomes weaker (Fig. 16). Figure 17 shows the temperature dependence of the scattering at $(0.5,0.5,0)$ and $(0.5,1.5,0)$ for
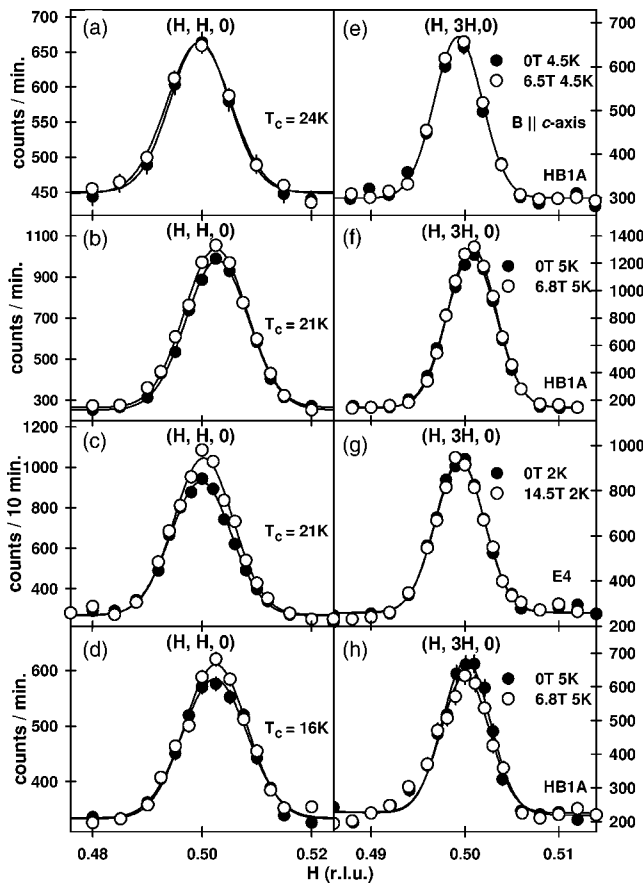
FIG. 15. The effect of a c-axis-aligned magnetic field on various SC PLCCO samples at low temperatures. The data below 7 T were taken at HB-1A of HFIR while higher field data were collected on E4 of HMI. The $[H,H,0]$ scans around $(0.5,0.5,0)$ for (a) T_c =24 K, (b),(c) 21 K, and (d) 16 K PLCCO samples at specified temperatures. (e)–(h) $[H,3H,0]$ scans around $(0.5,1.5,0)$ in the same experimental setup as in (a)–(d).
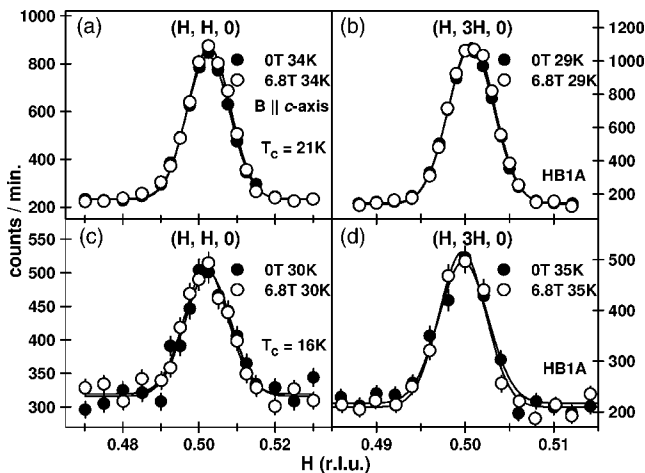

FIG. 16. The field dependence of the scattering across $(0.5,0.5,0)$ and $(0.5,1.5,0)$ at temperatures above T_c and below T_N. (a) and (b) for the T_c=21 K sample. (c) and (d) for the T_c=16 K sample. No field-induced effects are observed.

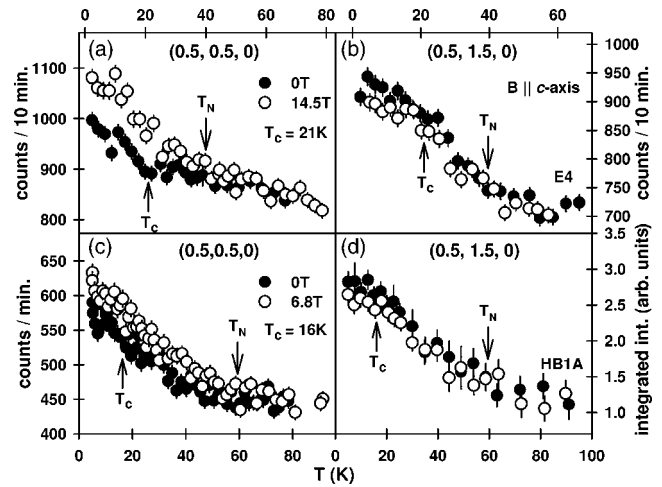

FIG. 17. Temperature dependence of the scattering at the $(0.5,0.5,0)$ and $(0.5,1.5,0)$ positions for (a) and (b) T_c=21 K and (c) and (d) T_c=16 K samples at zero and finite c-axis-aligned magnetic fields. Clear low-temperature field-induced effects are seen at $(0.5,0.5,0)$ but not at $(0.5,1.5,0)$ for both the T_c=21 K and 16 K PLCCO samples.

the T_c=21 K and 16 K samples at different fields. For the AF 3D ordered Bragg peak $(0.5,1.5,0)$, the intensity simply drops with increasing temperature and shows essentially no difference between field on and field off. On the other hand, scattering at $(0.5,0.5,0)$ shows clear low-temperature enhancement under field that vanishes at high temperatures. Although most of the field-induced effects occur at temperatures below the zero-field T_c as marked, we were unable to map out the detailed temperature-field dependence of the effect due to weakness of the signal. This is similar to the field-induced effect on incommensurate SDW in LSCO (Ref. 11) and La_2CuO_{4+y}.[13]

Finally, we carried out a series of $[H,H,0]$ and $[H,3H,0]$ scans across $(0.5,0.5,0)$ and $(0.5,1.5,0)$, respectively, for the T_c=21 K sample to determine the low-temperature field dependence of the scattering (Fig. 18). The open circles show the ORNL data taken at 5 K for fields up to 6.8 T while the filled circles are HMI data at 2 K for fields up to 14.5 T. The integrated intensity of the SDW at each field is computed by fitting the raw data with a Gaussian on a linear background (see Fig. 15). By combining ORNL and HMI data, we find that the field-induced effect at $(0.5,0.5,0)$ increases linearly with increasing magnetic field up to 13.5 T and may saturate at higher fields [Fig. 18(a)]. On the other hand, the 3D AF residual order $(0.5,1.5,0)$ peak of the T_c=21 PLCCO shows no observable field-induced effect for fields up to 14.5 T [Fig. 18(b)].

E. Magnetic field-induced anisotropy on the T_c=21 K superconducting $Pr_{0.88}LaCe_{0.12}CuO_{4\pm\delta}$

The discovery of a c-axis field-induced effect unrelated to the $(Pr,La,Ce)_2O_3$ impurity phase in underdoped PLCCO is suggestive but not a proof that such effect is related to the suppression of superconductivity, as one might argue that the AF phase in the SC PLCCO is somehow different from those
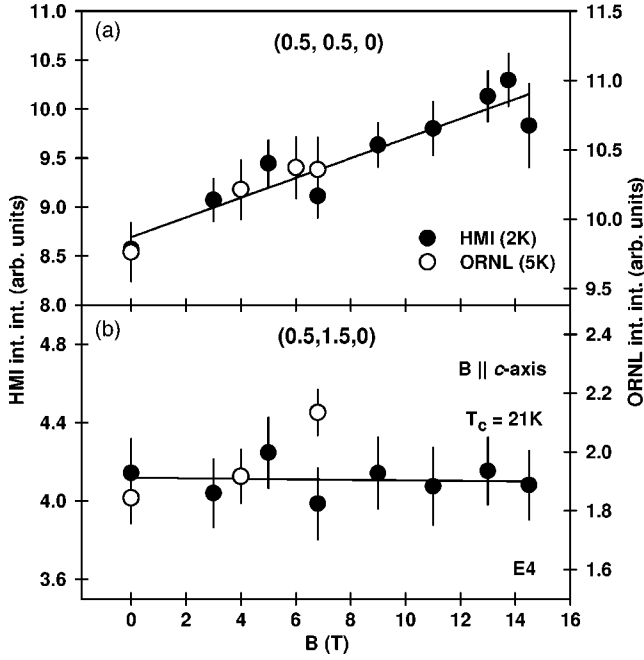
FIG. 18. (a) Integrated intensity of (0.5,0.5,0) as a function of increasing field. Open circles are data from ORNL at 5 K and filled circles are HMI data at 2 K. (b) Integrated intensity of (0.5,1.5,0) is independent of applied field up to 14.5 T.
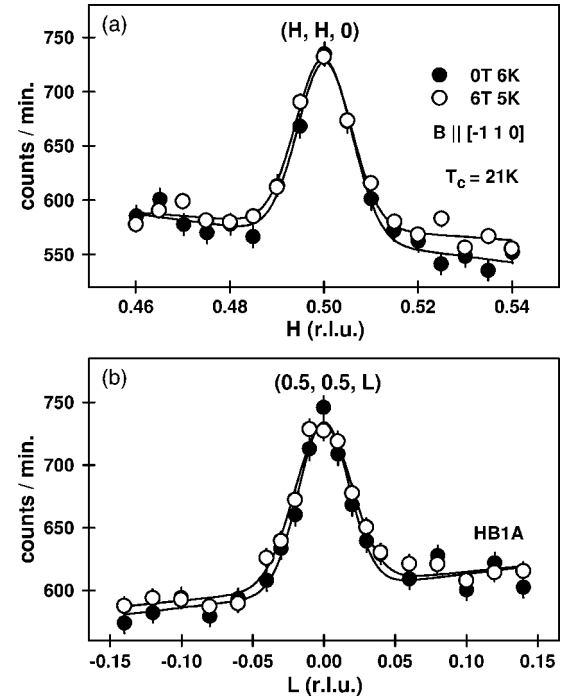

FIG. 19. The influence of an in-plane magnetic field on the SDW order in the T_c=21 K SC PLCCO. (a) $[H,H,0]$ scan around (0.5,0.5,0) for zero and 6 T at 5 K. (b) $[0.5,0.5,L]$ scan around (0.5,0.5,0). A 6 T in-plane magnetic field has no observable effect on the SDW order at 5 K. The c-axis coherence length of (0.5,0.5,0) is about 200 Å.

in NSC samples.[46] One way to check whether the observed effect is indeed related to the suppression of superconductivity is to determine its field directional dependence. Since high-T_c superconductors are layered materials, a magnetic field aligned along the c axis suppresses superconductivity much more dramatically than the same field parallel to the CuO$_2$ planes.

To compare the in-plane and c-axis magnetic field-induced effect, we focus on the SDW at (0.5,0.5,0) for the T_c=21 K PLCCO. Figure 19 shows scans along the $[H,H,0]$ and $[0.5,0.5,L]$ directions across (0.5,0.5,0) at zero and 6 T $\mathbf{B}\|[\bar{1},1,0]$ in-plane field. There is no observable field-induced effect, in contrast to c-axis field data across (0.5,0.5,0) [Figs. 15(b) and 15(c)]. On increasing the in-plane applied field to 14 T, we again failed to observe any field-induced effect around (0.5,0.5,0) at 5 K [Figs. 20(b) and 20(c)]. For comparison, we replot the data of Fig. 15(c) in Fig. 20(a). It is clear that a c-axis-aligned field enhances scattering at (0.5,0.5,0) while the same field parallel to the CuO$_2$ planes does not. Since a 14 T in-plane field only induces the spin-flop transition and does not affect the Cu/Pr moments of the residual AF phase, our observation of an anisotropic field effect in the T_c=21 K PLCCO is the most direct evidence that the enhancement of SDW order is related to the suppression of superconductivity.

The presence of a field-induced effect at the (0.5,0.5,0) SDW position but not at the AF (0.5,1.5,0) Bragg position suggests that Cu spins contributing to the diffusive SDW cannot arise from the same Cu spins giving the 3D AF moments. While similar field-induced enhancement was also observed in the case of optimally doped NCCO,[40] there are important differences between PLCCO and NCCO. First, op-

timally doped PLCCO has no residual AF order while 3D AF order coexists with superconductivity in NCCO even for samples with the highest T_c.[61] In addition, there are no detailed studies on how NCCO is transformed from an AF insulator to an optimally doped superconductor. As a consequence, it is unclear how to compare PLCCO directly with NCCO. Second, a c-axis-aligned field applied on the optimally doped NCCO not only enhances the magnetic signal at (0.5,0.5,0), but also at AF Bragg positions such as (0.5,1.5,0) and (0.5,0.5,3).[41] For underdoped PLCCO, a 14 T field has no observable effect on (0.5,1.5,0) AF 3D order. Finally, a c-axis-aligned field enhances the intensity of the Bragg peak at (1,1,0) for both NSC and SC NCCO (Ref. 41), while a similar field has no observable effect on any nuclear Bragg peaks in NSC and SC PLCCO. This difference must arise from the polarization of the Nd^{3+} ions in NCCO and therefore may not be intrinsic to the physics of electron-doped copper oxides.

IV. DISCUSSION

We use neutron scattering to study the phase transition of PLCCO from a long-range ordered antiferromagnet to a high-T_c superconductor without static AF order.[36] In the underdoped regime, we observe the coexistence of a quasi-2D SDW and a 3D AF order in the superconducting state. The 3D AF order has the same noncollinear magnetic structure as that in undoped Pr$_2$CuO$_4$ [Fig. 2(a)]. Since the noncollinear
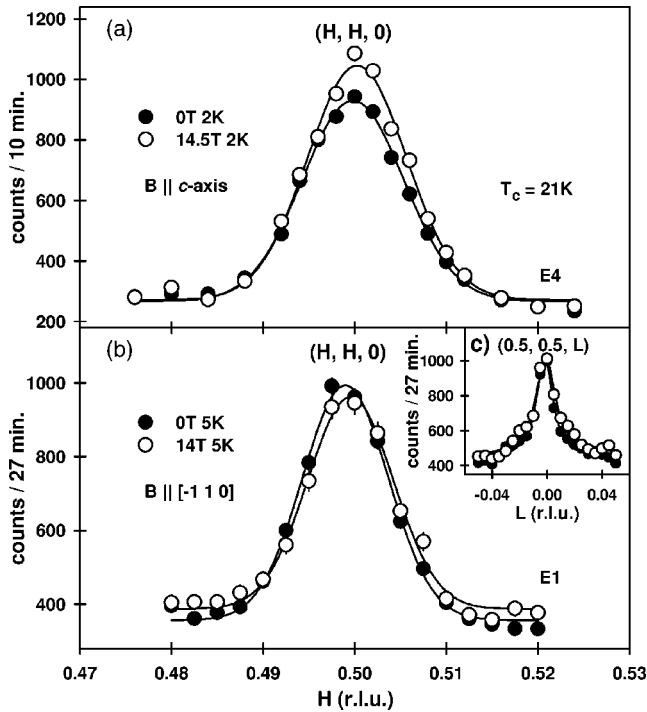
FIG. 20. Anisotropic field-induced effect on the SDW order of the $T_c = 21$ K PLCCO by a c-axis-aligned magnetic field and an ab-plane magnetic field. (a) $[H,H,0]$ scan across (0.5,0.5,0) with zero and 14.5 T field at 2 K in the $[H,K,0]$ zone. (b) $[H,H,0]$ scan across (0.5,0.5,0) with a $\mathbf{B} \parallel ab$-plane magnetic field at zero and 14 T. (c) $[0.5,0.5,L]$ scan across (0.5,0.5,0) with zero and 14 T at 5 K.

spin structure does not allow magnetic Bragg scattering at (0.5,0.5,0), it is interesting to ask whether the Cu spins giving rise to the 3D AF order also contribute to the diffusive quasi-2D scattering.

In one picture, the annealing process necessary for producing superconductivity in PLCCO may also induce macroscopic oxygen inhomogeneities, giving rise to mesoscopic separation between the SC and AF NSC phases. In the AF NSC phase, a weak random rotation of the magnetic moment from one plane to another induces a long-range spin order in the plane, but along the c axis one observes simultaneously a Bragg peak and a diffusive scattering. If both the diffusive (0.5,0.5,0) and 3D AF (0.5,1.5,0) signals are from the same Cu^{2+} spins macroscopically phase separated from nonmagnetic SC regions, one would expect that application of a c-axis-aligned magnetic field will have no (or the same) effect on both the 2D and 3D scattering. Instead, we find a clear c-axis field-induced effect at (0.5,0.5,0) but not at (0.5,1.5,0) (see Sec. III D). Therefore, Cu^{2+} spins contributing to the diffusive scattering cannot arise from the same Cu^{2+} spins giving 3D AF moments.

Alternatively, the annealing process may produce local oxygen distribution fluctuations acting as pinning centers for microscopic electronic phase separation. In this case, the quasi-2D AF scattering may arise from weakly correlated CuO_2 layers with a checkerboard AF order in the matrix of the 3D AF state. The observed diffusive commensurate SDW in PLCCO is then analogous to the incommensurate 2D
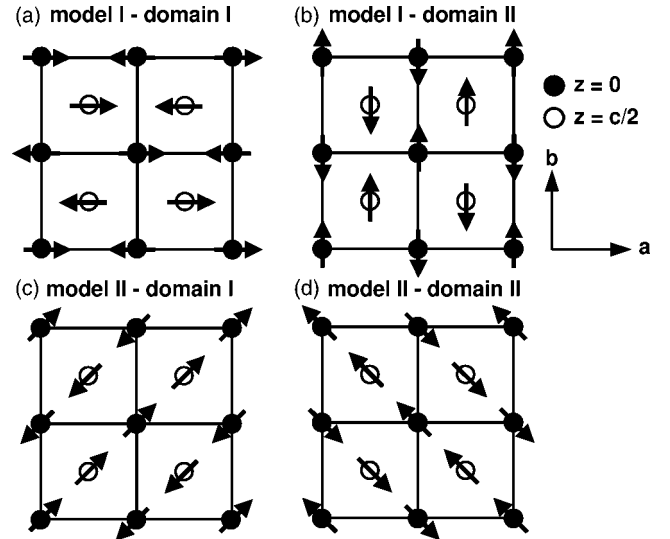

FIG. 21. Possible Cu^{2+} magnetic structures responsible for the SDW order. (a) and (b) Collinear spin model I, domains I and II. (c) and (d) Collinear spin model II, domains I and II. In collinear spin structures, the moments are in the ab plane. The closed and open circles represent the $z=0$ and $z=c/2$ CuO_2 planes, respectively. The Pr^{3+} spins are not shown, since the induced moment of Pr^{3+} is negligible in the SC PLCCO samples. Here we assumed weak (2 or 3 lattices) spin correlations along the c axis. Experimentally, we probably cannot distinguish such scattering from that of random 2D sheets in the 3D AF matrix.

SDW in hole-doped LSCO and La_2CuO_{4+y}.[4,5] When a c-axis-aligned magnetic field is applied, the residual 3D AF order is not disturbed but the diffusive SDW at (0.5,0.5,0) is enhanced at the expense of superconductivity. To estimate an effective moment of the 2D SDW order, we assume two models of spin structures in Fig. 21 that can give magnetic scattering at (0.5,0.5,0). Of course, we do not know the stability of the proposed spin structures in the tetragonal PLCCO unit cell and cannot determine the location of the Cu spins that contribute to the quasi-2D and 3D AF responses because neutrons are a bulk probe. Our purpose of introducing these models is to estimate an average Cu moment by normalizing the magnetic intensity at (0.5,0.5,0) to the weak nuclear (1,1,0) reflection. To estimate the effective Cu^{2+} moment at zero and 14.5 T, we first determine the magnitude of magnetic scattering at zero field by subtracting the integrated intensity of (0.5,0.5,0) at high temperatures from that at 2 K. The total magnetic scattering at 14.5 T is also determined by subtracting the high temperature nonmagnetic structural peak from that at 2 K. For $T_c = 21$ K PLCCO at 2 K, the integrated magnetic intensities at zero and 14.5 T are 2.0528 and 3.3411, respectively. This means that a 14.5 T field enhances the magnetic scattering at (0.5,0.5,0) by more than 60% $[I(14.5 \text{ T})/I(0 \text{ T}) = 1.66]$, much larger than the raw data in Figs. 15 and 16 would suggest. On the same incident beam monitor count, the integrated intensity of (1,1,0) nuclear Bragg peak is 4547.

Assuming each collinear model has two equally populated domains as depicted in Fig. 21 and negligible Pr moment contribution, we can calculate the expected magnetic inten-

TABLE II. Magnetic neutron scattering intensity calculations for proposed spin structures in Fig. 21. The angle θ is the scattering angle for the Bragg peak. $I_{cal}(0.5,0.5,0)/I_{cal}(1,1,0) = I_{ob}(0.5,0.5,0)/I_{ob}(1,1,0) = 2.7415 \cdot (0.939 M_{cu})^2/5.6531 = 2.0528/4547$ at 0 T, and $3.3411/4547$ at 14.5 T using spin structure I.

(H,K,L)	$I_{model\ I}$ (domains I and II)
$(0.5,0.5,0)$	$\dfrac{1}{2\sin 2\theta}32.0(\gamma e^2/2mc^2)^2(f_{cu}M_{cu}-0.88f_{pr}M_{pr})^2$
$(0.5,1.5,0)$	$\dfrac{1}{2\sin 2\theta}6.4(\gamma e^2/2mc^2)^2(f_{cu}M_{cu}-0.88f_{pr}M_{pr})^2$
(H,K,L)	$I_{model\ II}$ (domains I and II)
$(0.5,0.5,0)$	$\dfrac{1}{2\sin 2\theta}64.0(\gamma e^2/2mc^2)^2(f_{cu}M_{cu}-0.88f_{pr}M_{pr})^2$
$(0.5,1.5,0)$	$\dfrac{1}{2\sin 2\theta}12.8(\gamma e^2/2mc^2)^2(f_{cu}M_{cu}-0.88f_{pr}M_{pr})^2$
(H,K,L)	$I_{structural}$ in magnetic unit cell
$(1,1,0)$	$\dfrac{1}{\sin 2\theta}64.0(0.88b_{Pr}+b_{La}+0.12b_{Ce}+b_{Cu}-4b_O)^2$

TABLE III. Magnetic structure factor calculation for noncollinear spin structure of NCCO (type I/III) and PLCCO.

(H,K,L)	$(F)^2$ for NCCO type I/III
$(0.5,1.5,0)$	$25.6(\gamma e^2/2mc^2)^2(f_{cu}M_{cu}+1.85f_{nd}M_{nd})^2$
$(0.5,0.5,3)$	$32.0(\gamma e^2/2mc^2)^2(f_{cu}M_{cu}+1.7426f_{nd}M_{nd})^2$
(H,K,L)	$(F)^2$ for PLCCO
$(0.5,1.5,0)$	$25.6(\gamma e^2/2mc^2)^2(f_{cu}M_{cu}-0.88f_{pr}M_{pr})^2$
$(0.5,0.5,3)$	$32.0(\gamma e^2/2mc^2)^2(f_{cu}M_{cu}-0.8196f_{pr}M_{pr})^2$

sities of these two models in Table II. For the collinear model I with domains I/II [Figs. 21(a) and 21(b)], we obtain the Cu moment $0.032\mu_B$ at 0 T and $0.041\mu_B$ at 14.5 T. The enhancement of spin correlations appears mostly at $(0.5,0.5,0)$ and the intensity at $(0.5,1.5,0)$ is about 16 times smaller $[I(0.5,1.5,0)/I(0.5,0.5,0)=0.06$, here we used θ calculated for $E_i=E_f=13.7$ meV]. This is consistent with our observation of a weak (or no) field-induced effect at $(0.5,1.5,0)$. The collinear model II with domains I/II are essentially the same as that of the model I, except the spin directions are along the $[1,1,0]$ and $[\bar{1},1,0]$ directions [Figs. 21(c) and 21(d)]. This structure gives Cu moments of $0.022\mu_B$ at 0 T and $0.028\mu_B$ at 14.5 T. Therefore, the field-induced enhancement of the Cu moment is smaller ($\sim 0.006\mu_B$) than that of hole-doped LSCO and LCO in these two models.[11,12]

When as-grown PLCCO is transformed from a long-range ordered antiferromagnet to a high-T_c superconductor by annealing in pure Ar, the 3D AF order is degraded and a quasi-2D SDW order develops with the appearance of superconductivity. As optimal superconductivity is reached with $T_c=24$ K, both static 3D AF and diffusive SDW orders vanish. We confirm that the annealing process necessary for producing superconductivity also induces the bixbyite

$(Pr,La,Ce)_2O_3$ as an impurity phase. However, in contrast to $(Nd,Ce)_2O_3$ in SC NCCO, a 14 T field cannot polarize Pr^{3+} in $(Pr,La,Ce)_2O_3$ and this property therefore allows an unambiguous identification of the intrinsic field-induced effect on PLCCO. At optimal doping, a 6.5 T c-axis-aligned field does not induce static AF order due to the presence of a spin gap.[48] For underdoped materials, a 14 T c-axis field enhances the SDW at $(0.5,0.5,0)$ but has no observable effect on 3D residual AF order at $(0.5,1.5,0)$. A similar field applied along the $[\bar{1},1,0]$ direction in the CuO_2 plane only induces a spin-flop transition but has no effect on the SDW order. This is the most direct evidence that the enhancement of SDW is associated with the suppression of superconductivity.

While our results for optimally doped PLCCO are consistent with that for an overdoped PLCCO by Fujita *et al.*,[48] we cannot confirm their results for the $x=0.11$ ($T_c=25$ K) PLCCO. In particular, the 3D AF order has no observable field dependence in our underdoped samples. On the other hand, it would also be interesting to check if their $x=0.11$ PLCCO sample has a field-induced effect at $(0.5,0.5,0)$. At present, it is unclear how to reconcile our results with that of Fujita *et al.*[48] Perhaps the differences in Ce concentration and/or post annealing oxygen treatment plays an important role in determining the properties of these materials. In any case, what is clear is that underdoped PLCCO has a field-induced effect unrelated to the impurity phase, and such an effect appears to be associated with the suppression of superconductivity.[42]

To determine the influence of an applied field on the residual 3D AF order in SC electron-doped cuprates, one must understand the differences in the field-induced effect between optimally doped NCCO and underdoped PLCCO. The optimally doped NCCO shows clear c-axis field-induced effects at the 3D AF ordering positions such as $(0.5,1.5,0)$ and $(0.5,0.5,3)$. On the other hand, we were unable to find clear field-induced effects at $(0.5,1.5,0)$ for underdoped PLCCO. This difference may arise from the different rare-earth moment contributions to the magnetic scattering. For NCCO, the structure factor calculations in Table III show that the enhanced Nd^{3+} moment from the exchange coupling to the field-induced Cu^{2+} moment contributes constructively to the $(0.5,1.5,0)$ and $(0.5,0.5,3)$ reflections. On the other hand, the Pr^{3+} induced moment contributes destructively to the Cu^{2+} moment in PLCCO. As a consequence, any field-induced Pr^{3+} moment should reduce the scattering intensity at $(0.5,1.5,0)$ for PLCCO while a small Cu^{2+} moment enhance-

ment will induce large intensity enhancement at (0.5,1.5,0) and (0.5,0.5,3) for NCCO. Since SC PLCCO has a negligible field-induced Pr^{3+} moment, a small field-induced enhancement in the Cu^{2+} moment may not be easily observable at (0.5,1.5,0).

Our results can be thought of as analogous to that in hole-doped LSCO. When superconductivity first emerges in LSCO with increasing Sr-doping, quasi-2D incommensurate SDW peaks also appear spontaneously to coexist with super-conductivity as shown in Fig. 1(b).[7–9] As LSCO becomes an optimally doped superconductor, the static SDW is replaced by a spin gap and incommensurate spin fluctuations at energies above the gap.[6] A c-axis-aligned magnetic field that strongly suppresses superconductivity also enhances the static SDW order in underdoped LSCO (Refs. 10 and 11) and induces states within the gap in optimally doped LSCO.[14,15] Very recently, Khaykovich et $al.$[62] report the observation of a magnetic-field-induced transition between magnetically disordered and ordered phases in slightly underdoped LSCO with $x=0.144$. Here, static incommensurate SDW order can be induced directly by a field from the sample without zero-field SDW order.

For electron-doped PLCCO, we also find the simultaneous appearance of a quasi-2D SDW order and superconductivity, except in this case the SDW modulations are commensurate with the underlying lattice [Fig. 1(a)].[36] Similar to LSCO, optimally doped PLCCO also does not exhibit static SDW order. Work is currently underway to determine the size of the spin gap and spin fluctuations at high energies. When a c-axis-aligned magnetic field is applied, the static commensurate SDW order is enhanced for underdoped PLCCO but not for optimally doped samples. These results are very similar to hole-doped LSCO, thus suggesting the universality of the magnetic properties in both hole- and electron-doped cuprates. In the coming years, neutron scattering experiments will be carried out to search for the spin excitations in optimally and underdoped PLCCO. Our ultimate goal is to determine whether magnetism plays a fundamental role in controlling the properties of doped cuprates and the mechanism of high-T_c superconductivity.

V. SUMMARY AND CONCLUSIONS

We have systematically investigated the effect of a magnetic field on electron-doped PLCCO materials from an AF insulator to an optimally doped superconductor. By controlling the annealing temperatures, we obtain PLCCO samples with different T_c's and T_N's. When superconductivity first appears in PLCCO, a quasi-2D SDW order is also induced at (0.5,0.5,0), and both coexist with the residual 3D AF state.

While the annealing process also induces cubic $(Pr,La,Ce)_2O_3$ as an impurity phase similar to $(Nd,Ce)_2O_3$ in SC NCCO, we show that a magnetic field up to 14 T does not induce magnetic scattering in this impurity phase. To determine whether AF order is a competing ground state for superconductivity in electron-doped superconductors, we first must understand the influence of a magnetic field on the residual AF order for SC and NSC PLCCO without the complication of superconductivity. We confirm that a c-axis-aligned magnetic field has no effect on the AF order in the NSC PLCCO. Because PLCCO is a layered superconductor with highly anisotropic B_{c2}, superconductivity can be dramatically suppressed by a $\mathbf{B} \| c$-axis field but is much less affected by the same field in the CuO_2 plane. Utilizing this property, we determine the influence of an in-plane magnetic field on the residual AF order in SC PLCCO. We find that a 14 T field along the $[\bar{1},1,0]$ direction only cause a spin-flop transition but does not induce additional moments on Cu^{2+} and/or Pr^{3+} site in the SC PLCCO's. This suggests that the residual AF order in SC PLCCO behaves in a similar way as AF order in NSC materials.

To study the magnetic field effect on SDW modulations in SC PLCCO, we conducted experiments in two ways. First, we aligned the crystal in the $[H,K,0]$ geometry and applied magnetic field along the c axis. For both $T_c=21$ K and 16 K PLCCO samples, the c-axis-aligned field enhances the SDW order at the (0.5,0.5,0) position but has no observable effect at the 3D AF order position (0.5,1.5,0). The field-induced enhancement at (0.5,0.5,0) increases with increasing magnetic field up to 13.5 T for the $T_c=21$ K sample. The $T_c=16$ K sample also shows a field-induced effect at (0.5,0.5,0) for measured fields up to 6.8 T. Second, the crystal was aligned in the $[H,H,L]$ scattering plane and a magnetic field was applied along the $[\bar{1},1,0]$ direction. In this scattering geometry, both $[0.5,0.5,L]$ and $[H,H,0]$ radial scans around the (0.5,0.5,0) position in the CuO_2 plane show no observable field-induced effect. This anisotropy of a field effect confirms that the enhancement of SDW in the c-axis field direction is related to the suppression of superconductivity.

*Electronic address: daip@ornl.gov

[1] M. A. Kastner, R. J. Birgeneau, G. Shirane, and Y. Endoh, Rev. Mod. Phys. **70**, 897 (1998).

[2] S. Sachdev and S.-C. Zhang, Science **295**, 452 (2002).

[3] B. G. Levi, Phys. Today **57**, 24 (2004).

[4] H. Kimura, K. Hirota, H. Matsushita, K. Yamada, Y. Endoh, S.-H. Lee, C. F. Majkrzak, R. Erwin, G. Shirane, M. Greven, Y. S. Lee, M. A. Kastner, and R. J. Birgeneau, Phys. Rev. B **59**, 6517

(1999).

[5] Y. S. Lee, R. J. Birgeneau, M. A. Kastner, Y. Endoh, S. Wakimoto, K. Yamada, R. W. Erwin, S.-H. Lee, and G. Shirane, Phys. Rev. B **60**, 3643 (1999).

[6] K. Yamada, C. H. Lee, K. Kurahashi, J. Wada, S. Wakimoto, S. Ueki, H. Kimura, Y. Endoh, S. Hosoya, G. Shirane, R. J. Birgeneau, M. Greven, M. A. Kastner, and Y. J. Kim, Phys. Rev. B **57**, 6165 (1998).

[7] S. Wakimoto, G. Shirane, Y. Endoh, K. Hirota, S. Ueki, K. Yamada, R. J. Birgeneau, M. A. Kastner, Y. S. Lee, P. M. Gehring, and S. H. Lee, Phys. Rev. B **60**, R769 (1999).

[8] M. Fujita, K. Yamada, H. Hiraka, P. M. Gehring, S. H. Lee, S. Wakimoto, and G. Shirane, Phys. Rev. B **65**, 064505 (2002).

[9] M. Matsuda, M. Fujita, K. Yamada, R. J. Birgeneau, Y. Endoh, and G. Shirane, Phys. Rev. B **65**, 134515 (2002).

[10] S. Katano, M. Sato, K. Yamada, T. Suzuki, and T. Fukase, Phys. Rev. B **62**, R14677 (2000).

[11] B. Lake, H. M. Ronnow, N. B. Christensen, G. Aeppli, K. Lefmann, D. F. McMorrow, P. Vorderwisch, P. Smeibidl, N. Mangkorntong, T. Sasagawa, M. Nohara, H. Takagi, and T. E. Mason, Nature (London) **415**, 299 (2002).

[12] B. Khaykovich, Y. S. Lee, R. Erwin, S.-H. Lee, S. Wakimoto, K. J. Thomas, M. A. Kastner, and R. J. Birgeneau, Phys. Rev. B **66**, 014528 (2002).

[13] B. Khaykovich, R. J. Birgeneau, F. C. Chou, R. E. Erwin, M. A. Kastner, S.-H. Lee, Y. S. Lee, P. Smeibidl, P. Vorderwisch, and S. Wakimoto, Phys. Rev. B **67**, 054501 (2003).

[14] B. Lake, G. Aeppli, K. N. Clausen, D. F. McMorrow, K. Lefmann, N. E. Hussey, N. Mangkorntong, N. Nahara, H. Takagi, and T. E. Mason, Science **291**, 1759 (2001).

[15] J. M. Tranquada, C. H. Lee, K. Yamada, Y. S. Lee, L. P. Regnault, H. M. Ronnow, Phys. Rev. B **69**, 174507 (2004).

[16] B. Lake, K. Lefmann, N. B. Christensen, G. Aeppli, D. F. McMorrow, P. Vorderwisch, P. Smeibidl, N. Mangkorntong, T. Sasagawa, M. Nohara, and H. Takagi (unpublished).

[17] Shou-Cheng Zhang, Science **275**, 1089 (1997).

[18] Daniel P. Arovas, A. J. Berlinsky, C. Kallin, and Shou-Cheng Zhang, Phys. Rev. Lett. **79**, 2871 (1997).

[19] Y. Zhang, E. Demler, and S. Sachdev, Phys. Rev. B **66**, 094501 (2002).

[20] D.-H. Lee, Phys. Rev. Lett. **88**, 227003 (2002).

[21] Y. Chen and C. S. Ting, Phys. Rev. B **65**, 180513 (R) (2002).

[22] S. A. Kivelson, D.-H. Lee, E. Fradkin, and V. Oganesyan, Phys. Rev. B **66**, 144516 (2002).

[23] J. X. Zhu, I. Martin, and A. R. Bishop, Phys. Rev. Lett. **89**, 067003 (2002).

[24] E. Demler, W. Hanke, and S.-C. Zhang, Rev. Mod. Phys. **76**, 909 (2004).

[25] Pengcheng Dai, H. A. Mook, G. Aeppli, S. M. Hayden, and F. Doğan, Nature (London) **406**, 965 (2000).

[26] H. A. Mook, Pengcheng Dai, S. M. Hayden, A. Hiess, J. W. Lynn, S.-H. Lee, and F. Dogan, Phys. Rev. B **66**, 144513 (2002).

[27] Y. Hidaka and M. Suzuki, Nature (London) **338**, 635 (1989).

[28] P. Fournier, P. Mohanty, E. Maiser, S. Darzens, T. Venkatesan, C. J. Lobb, G. Czjzek, R. A. Webb, and R. L. Greene, Phys. Rev. Lett. **81**, 4720 (1998).

[29] Y. Wang, S. Ono, Y. Onose, G. Gu, Y. Ando, Y. Tokura, S. Uchida, and N. P. Ong, Science **299**, 86 (2003).

[30] Y. Tokura, H. Takagi, and S. Uchida, Nature (London) **337**, 345 (1989).

[31] H. Takagi, S. Uchida, and Y. Tokura, Phys. Rev. Lett. **62**, 1197 (1989).

[32] J. S. Kim and D. R. Gaskell, Physica C **209**, 381 (1993).

[33] K. Kurahashi, H. Matsushita, M. Fujita, and K. Yamada, J. Phys. Soc. Jpn. **71**, 910 (2002).

[34] M. Fujita, T. Kubo, S. Kuroshima, T. Uefuji, K. Kawashima, K. Yamada, I. Watanable, and K. Nagamine, Phys. Rev. B **67**, 014514 (2003).

[35] Here we call the observed quasi-2D AF scattering spin density wave (SDW) because of its similarity to the quasi-2D AF scattering seen in hole-doped materials (Refs. 4 and 5).

[36] Pengcheng Dai, H. J. Kang, H. A. Mook, M. Matsuura, J. W. Lynn, Y. Kurita, S. Komiya, and Y. Ando, Phys. Rev. B **71**, 100502(R) (2005).

[37] K. Yamada, K. Kurahashi, Y. Endoh, R. J. Birgeneau, and G. Shirane, J. Phys. Chem. Solids **60**, 1025 (1999).

[38] K. Yamada, K. Kurahashi, T. Uefuji, M. Fujita, S. Park, S.-H. Lee, and Y. Endoh, Phys. Rev. Lett. **90**, 137004 (2003).

[39] M. Matsuda, S. Katano, T. Uefuji, M. Fujita, and K. Yamada, Phys. Rev. B **66**, 172509 (2002).

[40] H. J. Kang, Pengcheng Dai, J. W. Lynn, M. Matsuura, J. R. Thompson, Shou-Cheng Zhang, D. N. Argyriou, Y. Onose, and Y. Tokura, Nature (London) **423**, 522 (2003).

[41] M. Matsuura, Pengcheng Dai, H. J. Kang, J. W. Lynn, D. N. Argyriou, K. Prokes, Y. Onose, and Y. Tokura, Phys. Rev. B **68**, 144503 (2003).

[42] Han-Dong Chen, Congjun Wu, and Shou-Cheng Zhang, Phys. Rev. Lett. **92**, 107002 (2004).

[43] P. K. Mang, S. Larochelle, and M. Greven, Nature (London) **426**, 139 (2003).

[44] H. J. Kang, Pengcheng Dai, J. W. Lynn, M. Matsuura, J. R. Thompson, Shou-Cheng Zhang, D. N. Argyriou, Y. Onose, and Y. Tokura, Nature (London) **426**, 140 (2003).

[45] M. Matsuura, Pengcheng Dai, H. J. Kang, J. W. Lynn, D. N. Argyriou, Y. Onose, and Y. Tokura, Phys. Rev. B **69**, 104510 (2004).

[46] P. K. Mang, S. Larochelle, A. Mehta, O. P. Vajk, A. S. Erickson, L. Lu, W. J. L. Buyers, A. F. Marshall, K. Prokes, and M. Greven, Phys. Rev. B **70**, 094507 (2004).

[47] A. T. Boothroyd, S. M. Doyle, D. M. Paul, and R. Osborn, Phys. Rev. B **45**, 10075 (1992).

[48] M. Fujita, M. Matsuda, S. Katano, and K. Yamada, Phys. Rev. Lett. **93**, 147003 (2004).

[49] A. N. Lavrov, H. J. Kang, Y. Kurita, T. Suzuki, Seiki Komiya, J. W. Lynn, S.-H. Lee, Pengcheng Dai, and Yoichi Ando, Phys. Rev. Lett. **92**, 227003 (2004).

[50] X. F. Sun, Y. Kurita, T. Suzuki, Seiki Komiya, and Yoichi Ando, Phys. Rev. Lett. **92**, 047001 (2004).

[51] Wu Jiang, J. L. Peng, Z. Y. Li, and R. L. Greene, Phys. Rev. B **47**, 8151 (1993).

[52] P. G. Radaelli, J. D. Jorgensen, A. J. Schultz, J. L. Peng, and R. L. Greene, Phys. Rev. B **49**, 15322 (1994).

[53] A. Nath, N. S. Kopelev, V. Chechersky, J. L. Peng, R. L. Greene, O. Boem-hoan, M. I. Larkin, and J. T. Markert, Science **265**, 73 (1994).

[54] G. Riou, P. Richard, S. Jandl, M. Poirier, P. Fournier, V. Nekvasil, S. N. Barilo, and L. A. Kurnevich, Phys. Rev. B **69**, 024511 (2004).

[55] P. Richard, G. Riou, I. Hetel, S. Jandl, M. Poirier, and P. Fournier, Phys. Rev. B **70**, 064513 (2004).

[56] I. W. Sumarlin, J. W. Lynn, T. Chattopadhyay, S. N. Barilo, D. I. Zhigunov, and J. L. Peng, Phys. Rev. B **51**, 5824 (1995).

[57] We note that the calibration of the Cu^{2+} moment is based on normalizing magnetic scattering to the weak nuclear (1,1,0) Bragg peak without considering absorption and extinction effects. In addition, since neutrons are a bulk probe and we can only estimate the moment by assuming an average ordered moment on all Cu sites. The errors only represent statistical uncertainties in the calculation.

[58] S. Skanthakumar, J. W. Lynn, J. L. Peng, and Z. Y. Li, J. Appl. Phys. **73**, 6326 (1993).

[59] V. P. Plakhty, S. V. Maleyev, S. V. Gavrilov, F. Bourdarot, S. Pouget, and S. N. Barilo, Europhys. Lett. **61**, 534 (2003).

[60] S. L. Li, S. D. Wilson, D. Mandrus, B. R. Zhao, Y. Onose, Y. Tokura, and Pengcheng Dai, Phys. Rev. B **71**, 054505 (2005).

[61] Whether the 3D AF phase coexists with superconductivity macroscopically or microscopically in NCCO is still an open question. In addition, it is not clear why optimally doped NCCO has 3D AF order in coexistence with superconductivity while similar PLCCO does not.

[62] B. Khaykovich, S. Wakimoto, R. J. Birgeneau, M. A. Kastner, Y. S. Lee, P. Smeibidl, P. Vorderwisch, and K. Yamada, cond-mat/0411355 (unpublished).